Sulfur-rich deposits associated with the deep submarine volcano Fani Maoré support broad microbial sulfur cycling communities

Stéven Yvenou, Mélanie Le Moigne, Olivier Rouxel, Johanne Aubé, Blandine Trouche, Cécile Cathalot, Emmanuel Rinnert, Xavier Philippon, Sandrine Chéron, Audrey Boissier, et al.

Microbiome

RESEARCH

Open Access

Sulfur-rich deposits associated with the deep submarine volcano Fani Maoré support broad microbial sulfur cycling communities

Stéven Yvenou[1*], Mélanie Le Moigne[1], Olivier Rouxel[2], Johanne Aubé[1], Blandine Trouche[1], Cécile Cathalot[2], Emmanuel Rinnert[2], Xavier Philippon[1], Sandrine Chéron[2], Audrey Boissier[2], Vivien Guyader[2], Yoan Germain[2], Anne Godfroy[1], Erwan G. Roussel[1] and Karine Alain[1*]

Abstract

Background In 2018, the island of Mayotte located in the western Indian ocean, has experienced a seismo-volcanic crisis linked to the birth of an impressive intraplate submarine volcano at the east of the island. This volcano, named Fani Maoré, which has not yet been the subject of microbiological studies, triggered the largest submarine eruptive event ever recorded. Close to the volcano's summit is a singular meter-size structure containing abundant native sulfur mineralizations. While a wide variety of ecosystems, with more or less well documented microbial communities, are found in active volcanoes on the ocean floor, knowledge on microbial communities hosted in habitats such as sulfur-rich intraplate volcanoes, that are not located on hotspots, remains limited. Genome-resolved metagenomics, culture-based functional approaches, geochemical and mineralogical analyses were combined to characterize the geological and physico-chemical constraints of the environment surrounding the yellow deposit part of this hotspot volcano and the composition and functions of its microbial community.

Results Geological and geochemical analyses indicated that this volcanic habitat had high concentrations in various sulfur species, including native sulfur, hydrogen sulfide and sulfate. Twenty-three Metagenome Assembled Genomes (MAGs) belonging to 8 different bacterial phyla, mainly *Pseudomonadota, Bacteroidota* and *Campylobacterota*, were reconstructed from the sulfur-rich deposit and analyzed. The vast majority of MAGs encoded genes for complete sulfur cycling metabolic pathways, in particular sulfur oxidation. Estimation of the cultivable microbial fraction revealed a diversity of microorganisms, with high growth rates for sulfur reduction, sulfate reduction with dihydrogen, and sulfur oxidation. Sulfur compound (S^0, SO_3^{2-} and $S_2O_3^{2-}$) disproportionation was also observed in cultures. The versatile genus *Sulfurimonas* was prevalent in culture at 6 and 20 °C, in the presence of different sulfur redox couples.

Conclusions Microbial communities, including taxa commonly found in ridge hydrothermal systems, were composed of autotrophic, heterotrophic or mixotrophic taxa using a large range of electron donors and acceptors to fuel their catabolism, particularly sulfur compounds in all common oxidation states. They had the genetic potential and physiological capacity to carry out all the metabolic reactions of the microbial sulfur cycle using the abiotic sulfur compounds present in their habitat. Representatives of the *Sulfurimonas* genus were among the main

*Correspondence:
Stéven Yvenou
Steven.Yvenou@ifremer.fr
Karine Alain
Karine.Alain@univ-brest.fr
Full list of author information is available at the end of the article

chemoautotrophs, since they predominated in eleven different temperature-redox pair culture combinations. Based on the observations, a conceptual model was proposed to describe the interactions in this sulfur-rich deposit that may occur between the microorganisms, the physico-chemical conditions and the sulfur compounds supplied by the environment.

Keywords Submarine volcano, Sulfur cycle, *Sulfurimonas*, Metagenome, Native sulfur

Background

Submarine volcanoes are widespread on the ocean floor and account for about 75% of Earth's total volcanic activity [1]. They are an important source of gases, solutes, molten rocks, trace elements and heat from the mantle to the ocean, contributing to biological productivity of the oceans and providing mineral resources [2]. Volcanic eruptions also reshape the seafloor landscape and create new microbial habitats [3]. While microbial communities living in submarine hydrothermal vents at mid-ocean ridges (ridge volcanism) and back-arc basins (subduction zone volcanism) have been extensively studied (e.g., [4, 5]) and reviewed in several articles [6–9], microbes living in isolated intraplate submarine volcanoes remain poorly characterized, (e.g., [10]). Active intraplate volcanoes represent an excellent opportunity to study metabolic traits of microbial communities colonizing these newly formed habitats in an area usually devoid of any other active volcanic structures.

From May 2018 to 2021, the island of Mayotte (Comoros archipelago) has experienced a major seismo-volcanic crisis that came along with effusive eruptions [11]. This event represented the largest submarine eruption ever documented and has led to the birth of a new volcano named Fani Maoré [12] (Fig. 1). With a height of 936 m and a diameter of about 2 km, this intraplate volcano was located on the seafloor at 3300 m depth, about 50 km from the island of Mayotte on the East volcanic chain [11, 12]. From a magma chamber deeply buried in the Earth's mantle, this volcano has extruded more than ~5 km^3 of lava that caused the island of Mayotte to subside and move a few centimeters [11]. Following these events, the extensive survey and scientific studies showed that the earthquakes had a volcanic rather than a tectonic origin. Most studies performed so far have thus focused on the seismicity and microbathymetry of the area, as well as petrological and geochemical analyses of samples, in order to follow the evolution of the magma [11–14]. A

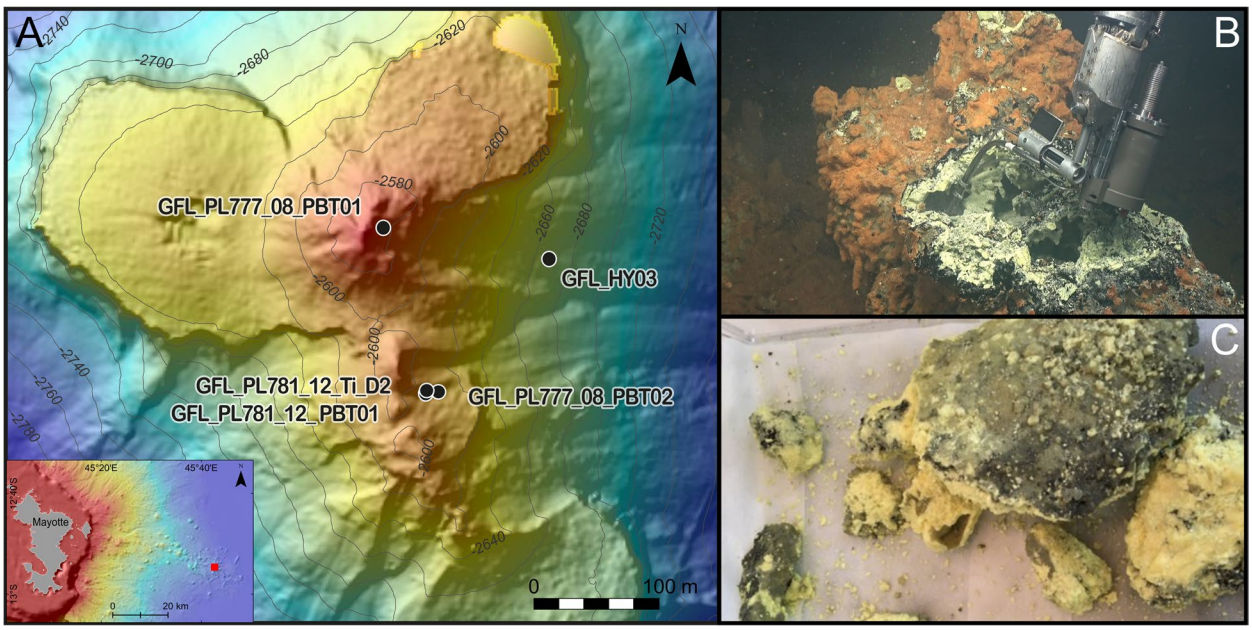

Fig. 1 **A** Bathymetric map of the Fani Maoré submarine volcano. The locations of the environmental sample collection points are indicated by black circles. **B** Photograph of the fluid sample collected inside the fractured cavity (GFL_781_12_Ti_D2). **C** Photograph of the sample GFL_PL781_12_PBT01 containing elemental sulfur particles

significant focus has also been directed to water column geochemical signatures in order to determine the impact of the eruptive and degassing activity on the water column at a local scale [15]. In the vicinity of the volcano's summit, a volcanic structure composed of accumulations of yellow brittle mineral grains of native sulfur and outer crust of black volcanic glass and fine iron-oxyhydroxide coating was easily distinguishable from other parts of the eruptive zone by an unusual columnar structure (Fig. 1).

In most mid-ocean ridge hydrothermal systems [6–9], various forms of sulfur compounds such as sulfate, sulfide, and iron-sulfide minerals are often abundant. Elemental sulfur is generally restricted to submarine volcanic systems (at back-arc basins, volcanic arcs and hotspots), as it can be formed by disproportionation of volcanic SO_2 [16–21]. The young volcanic structure of the Fani Maoré volcano represented a rare opportunity to study the deep-sea chemolithotrophic microbial sulfur cycle in an intraplate environment rich in native sulfur.

Previous studies of microbial communities in submarine volcanoes have shown that they are frequently colonised by generalist microorganisms including several genera of *Campylobacterota* (particularly of the genus *Sulfurimonas)* [3, 22]. *Campylobacterota* of the genera *Sulfurimonas* and *Sulfurovum* are widespread in redoxcline environments like deep-sea hydrothermal vents and sulfidic environments. They are physiologically versatile and can grow at low to warm temperatures, some having a fairly wide growth temperature gradient [6]. In sulfur-rich ecosystems, they can be predominant in various matrices (plumes, chimney walls, microbial mats) and are often among the earliest colonizers of uninhabited vent ecosystems [23–26]. For instance, *Candidatus (Ca.)* 'Sulfurimonas pluma' was found to be ubiquitous and abundant in cold oxygen-satured and hydrogen-rich hydrothermal plumes at mid-ocean ridges worldwide [26, 27]. Furthermore, in few hydrothermal plumes highly diluted in seawater, a dominance of seawater-ubiquitous microorganisms (such as SAR11 and SAR324) has been reported, as well as a lower proportion of subsurface microorganisms [28, 29].

The present study leveraged cultivation and metagenomic approaches to investigate the metabolic traits of microbial communities colonizing these newly-formed sulfur rich habitats, which were characterized by mineralogical and geochemical analyses. Overall, microbial taxonomic and functional diversity was inferred from metagenomes retrieved from an environmental sample and from dilution to extinction cultures targeting sulfur cycling metabolisms (sulfur disproportionation, sulfur oxidation, sulfur reduction and sulfate reduction) at 6 °C, 20 °C and 40 °C. Further phenotypic and metabolic characterization of sulfur cycling taxa were obtained from the analysis of metabolism substrates and products within cultures.

Based on the analysis of these results we highlighted the metabolic patterns of the microbial taxa that colonized this newly-formed, native-sulfur rich volcanic habitat, and presented a conceptual model of the sulfur cycle in this habitat and of its main microbial actors.

Methods

Sample collection

In May 2021, during the GEOFLAMME oceanographic cruise [30] onboard the research vessel *Pourquoi pas?*, volcanic rocks from the Fani Maoré volcano were collected using the Remotely Operated Vehicle (ROV) Victor 6000, at 2596 m below sea level and with an altitude of three meters above the seafloor (sample GFL_PL781_12_PBT01; 12° 54.724′ S–45° 42.728′ E [31]). Fragments of volcanic rocks, volcanoclastic deposits and Fe-oxyhydroxide-rich sediments were recovered at the top of the volcano (Fig. 1), together with a chimney-like deposit composed of yellow minerals resembling native sulfur and lining an open cavity. Solid samples were placed into a dedicated decontaminated insulated sample box (referred as PBT-box) and then brought back to the ship for subsampling, while fluids were recovered using titanium syringes (sample GFL_PL781_12_TiD2, Fig. 1B), as described in previous studies [32], and following a method adapted for low-temperature fluids (e.g., [33]). Due to a technical problem, temperature recording was not successful during the fluid collection. On board, immediately after sample recovery, samples for cultures were stored at 4 °C in sterile Schott bottles under a N_2 atmosphere, and samples for metagenomic analyses were stored at −80 °C.

Other volcanic rocks (sample GFL_PL777_08_PBT02) and reference background seawater (sample GFL_PL777_08_PBT01) were collected in PBT-boxes (Fig. 1A), and background seawater was also sampled using a Conductivity-Temperature-Depth (CTD) hydrocast (sample GFL_HY03_B01), before filtration (50 mL filtered with a 0.2-µm pore-size filter) (Fig. 1A).

Fluid chemistry

Fluids were processed on board straight away after recovery of the Ti-syringes using the following scheme:

(1) Aliquot was collected for shipboard pH and total $HS^- + H_2S$ analysis [34];
(2) Another aliquot was archived in 10 mL HDPE Nalgene flasks for on shore analysis by ionic chromatography (Thermo Scientific ICS-5000). Samples

were diluted by a factor of 500 according to the manufacturer's recommendations.
(3) The remaining fluid solution in the Ti-samples was then directly filtered from the Ti syringe through 0.45 µm pore-size online filter (Sterivex™) and the solution was transferred to an acid cleaned 1 L HDPE bottle. Because of the low-temperature nature of the sampled fluid (i.e., undistinguishable from background seawater, see results), recovered particles were considered to derive from the entrainment of surrounding mineral from the sulfur-rich structure rather than being precipitated after sampling as classically observed in hydrothermal fluids. Major and trace elements were then measured onshore on filtered and acidified aliquots (pH 1.8) by Inductively Coupled Plasma-Mass Spectrometry (ICP-MS) after a 100-fold dilution.

Upon recovery of the PBT-box containing fragments of sulfur-rich deposits and entrained background seafloor seawater, a strong H_2S odor was generated over time in the solution, suggesting active degassing of the minerals. This was later confirmed after recovering solid fragments that showed characteristic popping sounds upon drying.

Rock geochemistry and mineralogy

Fragments of sulfur-rich deposits recovered from the PBT-box were subsampled for further geochemical and petrographical studies. Samples were stored frozen until onshore processing. X-ray fluorescence (XRF) and X-ray diffraction (XRD) analyses were performed on bulk powder prepared after drying mm-size fragments in an air oven at 50 °C and powdered using an agate mortar. Mineralogical and quantitative chemical data were acquired using X-ray techniques. XRD analyses were conducted with a BRUKER AXS D8 ADVANCE diffractometer (a device type Bragg–Brentano equipped with a Cu X-ray tube, and the *VANTEC-1* Position Sensitive Detector with a nickel filter (Ni 0.5)). Samples were top loaded into 2.5-cm-diameter circular cavity holders, and analyses were run between 5° and 70° 2θ, in steps of 0.01° 2θ at 1 s/step, (40 kV, 30 mA). Minerals were identified using Diffrac suite EVA software. XRF analyses were conducted with a wavelength dispersive XRF spectrometer (WD-XRF; BRUKER AXS S8 TIGER) on fusion beads. After data acquisition, the measured net peak intensities, corrected for inter-element effects, were converted into concentrations using calibration curves generated from analysis of certified geochemical standard powders (measured under identical analytical conditions). Calibrations were established using a set of certified materials.

For sulfur isotopes, sample powder was digested in inverted aqua regia and then purified by elution through a cationic resin to remove any interfering matrix. The solution was analyzed by a Neptune™ multiple collector ICP-MS, following the procedure of [35] and calibrated against a set of internal and external standards (IAEA NZ-1, NZ-2, NZ-4, NBS 123).

Bulk and hand-picked chips were also analyzed for major and trace elements by High Resolution ICP-MS. Sample were dissolved in PTFE beaker on hot plate using an acid mixture of HF, HCl, and HNO_3. Digested samples were then diluted 5000-fold and analyzed by HR-ICP-MS following similar approaches than for fluid samples described above. A set of international georeference materials (e.g., BHVO-2, GH, UB-N, NOD-P-1, IF-G, NIST2711) and internal standard solutions relevant to sulfur-rich samples were used to calibrate the measurements.

DNA extraction and sequencing for metagenomics

Total DNA was extracted with a standard Phenol: Chloroform: Isoamyl Alcohol (25:24:1), pH 8, protocol [36], from 45 mL of a mixture composed of rocks, yellow sulfur particles and cavity's seawater, with the addition of 50 µM linear acrylamide to enhance nucleic acids precipitation (Invitrogen™). One negative control was processed in parallel. Elution of total DNA extracts was performed in 30 µL EB buffer (10 mM Tris–Cl, pH 8.5). Nucleic acid solution quality was determined using the NanoDrop™ 8000 (Thermo Scientific, Waltham, MA, USA) spectrophotometer. Double-strand DNA concentration was measured using the kit Quantifluor™ (Promega®) dsDNA system. Genomic DNA was then purified with QIAmp kit (Qiagen®) before libraries construction. DNA sample was sequenced by NovaSeq 6000 (2 × 150 bp, paired-end reads) technology by the Fasteris company (Plan-les-Ouates, Switzerland).

Sequence processing, assembly, and binning

Lack of adapter contamination in the demultiplexed raw reads was ascertained with FastQC [37] and MultiQC [38], before carrying out quality filtration with Illumina-Utils python scripts [39], following recommendations by Minoche et al. [40]. The following steps were performed with the help of the Snakemake workflows [41], available with Anvi'o v7 [42, 43]. Namely, reads were assembled using IDBA-UD (v1.1.3, [44]) with minimum contig length set at 1000 bp. Identification of Open Reading Frames (ORFs) in the contigs was done with Prodigal [45] and functional annotation obtained using KOfamscan [46]. After mapping of the short reads on the resulting contigs with bowtie2 [47, 48], metagenomic binning was performed with MetaBAT2 v2.15 [49], using default

parameters. The resulting bins were manually refined with the "anvi-refine" program from Anvi'o v7.1 [50]. The quality of these MAGs was first assessed using CheckM v1.2.0 [51] implemented on Anvi'o, with single prokaryotic marker genes, and only MAGs with more than 60% completion and less than 10% redundancy were retained for the next step. Next, the completion and redundancy of MAGs retained for further analysis were analysed in more detail on the MaGe platform with CheckM v2 [51] using lineage-specific markers. Taxonomic affiliation of the MAGs was determined with the classify workflow of the Genome Taxonomy Database GTDB-Tk v2.4.0 (reference data v09-RS220) [52].

The Average Nucleotide Identity (ANI; OrthoANIu) values were calculated on EzBioCloud [53] using the ANI calculator, with the orthologous genes of the closest relatives.

Data availability

This Whole Genome Shotgun project has been deposited at DDBJ/ENA/GenBank under the BioProject PRJNA938062, and accession numbers GCA_045047305.1, GCA_045047075.1, GCA_045047105.1, GCA_045047115.1, GCA_045047095.1, GCA_045047085.1, GCA_045046905.1, GCA_045046925.1, GCA_045046865.1, GCA_045046885.1, GCA_045046875.1, GCA_045046665.1, GCA_045046715.1, GCA_045046705.1, GCA_045046655.1, GCA_045046645.1, GCA_045107175.1, GCA_046055765.1, GCA_046055745.1, GCA_045267885.1, GCA_045107135.1, GCA_045267865.1, and GCA_045267845.1. 16S rRNA gene sequences of taxa cultivated by the approach derived from the most probable number method have been deposited at GenBank under the accession numbers PQ541048 to PQ541067. *Sulfurimonas* strains isolated in this study are stored at − 80 °C with 5% (v/v) dimethylsulfoxide.

Estimating microbial diversity in the sample

Microbial diversity in the sample was estimated both before and after assembly. Before assembly, Phyloflash v3.4 [54] was applied to the quality filtered reads to identify 16S rRNA genes fragments based on read identity with the SILVA v138.1 database [55], with default parameters and a clustering threshold of 100%. Shortly, Phyloflash maps reads to the reference database using BBMap [56] and extracts sequences based on a 70% minimum identity threshold. Additionally, it implements the SPAdes assembler [57] to attempt to reconstruct full-length 16S rRNA gene sequences. Sequences affiliated with Eukaryota, Mitochondria and Chloroplasts were then removed from the resulting table.

After assembly, the number of genomes present in the sample was estimated on the basis of the presence of specific HHM profiles of single-copy core genes from *Bacteria*, *Archaea* and *Protista* (HMM sources: Bacteria_71 for *Bacteria*, Archaea_76 for *Archaea;* Protista_83 for *Protista*; https://anvio.org/help/7/artifacts/hmm-source/). A taxonomic overview of the sample was then obtained based on the most abundant single-copy core gene, Ribosomal L16, using Anvi'o command *anvi-estimate-scg-taxonomy* in metagenome mode, computing gene coverages as an approximation of bacterial relative abundances. Visualization of the taxonomy results was done in R v3.6.1 (R Core Team, 2019), using packages phyloseq (v1.28.0 [58]) and ggplot2 (v3.3.0 [59]).

Phylogenomic tree and prediction of optimal growth temperature

A phylogenomic analysis was carried out with Anvi'o (v8), based on seventy-one single copy core genes present in *Bacteria* (Supplementary Table S1) (collection modified from [60]), by using the Anvi'o workflow for phylogenomics (https://merenlab.org/2017/06/07/phylogenomics/). For each MAG, three to six taxonomically close genomes/MAGs according to GTDB (https://gtdb.ecogenomic.org/) were chosen based on their quality for the phylogenomic analysis. The phylogenomic tree was constructed based on the seventy-one concatenated single-copy core genes of each MAGs and genomes using FastTree, implemented in the Anvi'o workflow for phylogenomics. To confirm the topology of this phylogenomic tree, a phylogenetic reconstruction based on the seventy-one concatenated single-copy core genes (aligned with MUSCLE v5.1) [61] was performed by maximum likelihood method using the IQ-TREE v2.0.3 software [62]. Branch support was computed with the aLRT SH-like method using 1000 replicates.

Prediction analysis of the optimal growth temperature was performed by running the package TOME (Temperature Optima for Microorganisms and Enzymes) (https://github.com/EngqvistLab/Tome) [63], based on 2-*mer* amino acid composition of the proteomes of the volcano MAGs and their closely related genomes/MAGs.

In addition, the taxonomic affiliation of *Sulfurimonas* MAGs was investigated in detail using GTDB-Tk's *classify* workflow (v2.4.0; GTDB reference tree 09-RS220). A phylogenomic analysis was performed with the closest MAGs and all cultivated species. To this end, the single copy-gene clusters present in all sequences were first extracted and concatenated using Anvi'o (v8), aligned with MUSCLE v5.1 [61], trimmed with trimAI v1.4.1 [64] and a phylogenetic reconstruction based on 250 concatenated single-copy gene clusters (Supplementary Table S2)

was performed by maximum likelihood method using the IQ-TREE v2.0.3 software [62], with 1000 iterations.

Metabolic pathway prediction

Metabolic pathway prediction was performed by combining results of various software/platforms to annotate the MAGs: Anvi'o (v7.1) (https://merenlab.org/tutorials/infant-gut/#chapter-v-metabolism-prediction), Prokka (v1.14.6) [65] (https://github.com/tseemann/prokka) and MaGe MicroScope (v3.16.0) (https://mage.genoscope.cns.fr/microscope/mage/index.php). The standard genetic code was used for all MAGs, except *Patescibacteria*_MAG21. For the latter, an alternative genetic code (code 25) was used because in the class "*Ca.* Gracilibacteria" of the *Patescibacteria*, the UGA codon codes for a glycine and not for a stop codon [66].

A first analysis was made with Anvi'o, with workflows for microbial pangenomics (https://merenlab.org/2016/11/08/pangenomics-v2/) and then for metabolic prediction (https://anvio.org/help/main/programs/anvi-estimate-metabolism/). Genes were first annotated with KEGG [67], and KOfams (a database of KEGG orthologs), and then for each MAG the presence of some enzyme-encoding genes and the completeness of few metabolic pathway was estimated.

To analyze the global metabolic potential, presence of key carbon fixation enzymes was sought and pathway completeness was observed for ATP synthesis/respiratory chain, carbohydrate metabolism and anaerobic respirations, using the Anvi'o workflow for pangenomics to identify functions and estimate metabolism, and these annotations were refined with MaGe and Prokka predictions. The completeness of metabolic pathways was mapped using Prism10 (GraphPad) software.

Next, a comprehensive study of dissimilatory reactions of the microbial sulfur cycle and organosulfur transformations was conducted, based on Prokka and MaGe annotations, and the presence of these pathways was compared with the metabolic prediction made with Anvi'o as described above. FeGenie v1.2 was used to identify iron genes and iron gene operons in MAGs using HMM-profiles [68]. In addition, DiSCo software was used to predict the metabolic function of the following proteins: dissimilatory sulfite reductase (DsrABC, DsrMKJOP, DsrD, DsrEFH, DsrL, DsrT), heterodisulfide reductase (HdrABC), quinone-interacting membrane bound oxidoreductase (QmoABC), sulfate adenylyltransferase (Sat), adenosyl phosphosulfate reductase (AprAB and AprM) [69]. Pathways in which these enzymes are involved have been described elsewhere [70, 71]. A map indicating the presence or the lack of each key enzyme of the microbial sulfur cycle was created with Prism10 (GraphPad) software.

Growing conditions for the different metabolisms of the sulfur cycle

To estimate the part of cultivable microorganisms involved in the microbial sulfur cycle, culture series were carried out targeting the four main metabolisms of the sulfur cycle: anaerobic sulfur disproportionation, sulfur reduction, sulfur oxidation, and sulfate reduction. For each catabolism, two different culture media were prepared as detailed below. Serial dilutions were performed in 50 mL serum vials filled with 9 mL of medium (41 mL of headspace) and closed with butyl stoppers and aluminum caps. For all culture conditions, the same mineral medium composed of (for 1 L) NaCl 25 g; $MgCl_2.6H_2O$ 4.4 g; NH_4Cl: 0.33 g; KCl: 0.50 g; $CaCl_2.2H_2O$ 0.33 g; KH_2PO_4: 0.33 g; 1 mL of trace elements (medium 141 from Deutsche Sammlung von Mikroorganismen und Zellkulturen (DSMZ) https://www.dsmz.de/microorganisms/medium/pdf/DSMZ_Medium141.pdf) and 1 drop of resazurine (corresponding to 0.5 $mg.L^{-1}$) was prepared. Then, the mineral base was boiled to remove part of the oxygen and 6.92 g of piperazine-*N*,*N*′-bis(2-ethanesulfonic acid) (PIPES buffer) were added, followed by 1 mL of vitamin solution (DSM medium 141). The pH was adjusted to 7 before closing the bottle and degassing the atmosphere by seven 45 s vacuum-gas (nitrogen 100%) cycles. With the exception of the sulfur oxidation media, media were reduced by adding 0.6 mM of $Na_2S.9H_2O$, from a 0.5 M solution at pH 7.

For each culture condition, one-tenth dilutions were made in five inoculated series, and one uninoculated serie as negative control, down to dilution 10^{-9}. Incubations were performed at 6 °C, 20 °C, and 40 °C. Each medium was autoclaved twice at 105 °C for 30 min (with 24 h delay between 2 cycles) before adding the final gas phase.

In the sulfur-reduction media, the mineral base was amended with 5 $g.L^{-1}$ elemental sulfur as the terminal electron acceptor. The first sulfur reduction condition was carried out with dihydrogen (H_2) as the electron donor (H_2/CO_2, 80/20% atmosphere, 200 kPa). The second sulfur reduction condition was based on a mixture of 20 amino acids (L-alanine, L-valine, DL-methionine, L-aspartic acid, L-leucine, L-phenylalanine, L-tryptophane, L-histidine, L-proline, L-serine, L-cysteine, L-tyrosine, L-glycine, L-glutamine, L-leucine, L-asparagine, L-lysine, L-glutamic acid, L-threonine, L-arginine, L-isoleucine all at 0.02% (w/v)) as energy and carbon sources (N_2 100% atmosphere, 200 kPa).

In the sulfate reduction media, the mineral base was amended with 10 mM sulfate (SO_4^{2-}) as the electron acceptor. In the first condition, H_2 was used as the electron donor and CO_2 as the carbon source (H_2/CO_2, 80/20% atmosphere, 200 kPa). In the second condition,

acetate (10 mM) was used as both electron donor and carbon source (N_2 100% atmosphere, 200 kPa).

In the sulfur oxidation media, elemental sulfur (S^0) at 5 g.L^{-1} was used as the electron donor in the first condition, and hydrogen sulfide at 3 mM (H_2S) was used as the electron donor in the second condition. For both media, dioxygen (O_2) at 3% (v/v, 200 kPa) in the gas phase and nitrate (NO_3^-) at 10 mM were used as terminal electron acceptors, and CO_2 at 97% (v/v, 200 kPa) was used as the carbon source.

In the anaerobic sulfur compound disproportionation media, S^0 at 5 g.L^{-1} was used as the sole electron donor/acceptor in the first condition, and both sulfite (SO_3^{2-}) at 5 mM and thiosulfate ($S_2O_3^{2-}$) at 10 mM were added in the second condition. These media were incubated under a 100% CO_2 atmosphere (200 kPa).

Growth monitoring of cultures

The cell density present in the natural sample was determined by cell counting (two replicates), using an epifluorescence microscope (Olympus® BX60, Olympus Corporation, Tokyo, Japan) after labelling the cells with acridine orange, as described elsewhere [72]. Cell number in the 10^{-1} and 10^{-2} dilution vials was also counted just after inoculation. During the incubations, to estimate growth in serum vials, in addition to observing turbidity, weekly microscopic observation (× 1000) (Olympus® BX60, Olympus Corporation, Tokyo, Japan) of 20 fields was performed, starting with the dilution 10^{-1} and continued in case of growth by counting the next dilution. The concentration of viable, cultivable microorganisms in the sample was estimated using a method derived from the most probable number approach [73], based on the dilution factor applied, the number of replicates and the number of vials in which growth was observed. These estimates were generated using a pre-formatted Excel spreadsheet published previously [73]. The cultivation percentage was calculated from the most probable number of viable and cultivable cells estimated for each catabolism and each temperature, in comparison with the number of cells counted in the natural sample.

Analysis of substrates and metabolic products

Volatile fatty acids (acetate, lactate, formate, and propionate), SO_4^{2-}, SO_3^{2-}, $S_2O_3^{2-}$, NO_3^-, and ammonium (NH_4^+) were monitored using ion chromatography (IC) as described previously [74, 75], with the following modifications. For IC analysis, 1 mL of culture was centrifuged at 15,000 × *g* for 10 min, then the supernatant was filtered (Millex Durapore® PVDF filter units, 13 mm, 0.22 µm; Millipore Corporation, MA, USA) and diluted one-tenth with filtered milliQ water into pyrolyzed chromacol™ vials (Thermo Scientific™, Loughborough, UK). Anion chromatography analyses were run on a Thermo Scientific™ Dionex™ ICS-6000 HPIC™, equipped with a microbore flow controller (1–3 mm column internal diameter), an ion exchange column (Dionex™ IonPac™ AG15 2 mm × 50 mm), coupled to a suppressor (Thermo Scientific™ Dionex™ ADRS™ 600 with KOH as eluent at 0.3 mL.min^{-1}). The gradient program was as follows: 8 mM KOH during 3 min; increase to 14 mM KOH during 12 min; increase to 17 mM KOH during 8 min; increase to 45 mM KOH during 0.5 min; increase to 48.20 mM KOH during 10.5 min; increase to 58 mM KOH during 6 min; increase to 80 mM KOH during 9.75 min; decrease to 8 mM KOH during 10 min. Cations were run on a Dionex™ EGC-500 equipped with two columns (CS16–4 µm and 1 CG16–4 µm), coupled to a suppressor (Thermo Scientific™ Dionex™ CDRS™ 600) with methane sulfonic acid as eluent. The gradient program was as follows: 9 mM methane sulfonic acid during 30 min; increase to 50 mM methane sulfonic acid during 23 min; decrease to 9 mM methane sulfonic acid during 7 min.

Dissolved sulfide was identified with the Cord-Ruwisch method, based on the colorimetric/spectrophotometric detection of a black FeS precipitate in the presence of H_2S, as described previously [76].

Identification of taxa present in the last positive dilutions

To determine the taxonomic affiliation of the microorganisms growing in the last dilutions for each condition, genomic DNA was extracted from 2 mL of culture by the Phenol:Chloroform:Isoamyl Alcohol (25:24:1, v/v) method. For *Bacteria*, the genes encoding 16S rRNAs were amplified by PCR using GoTaq® G2 DNA Polymerase (Promega) and the primers Bac8 F (5′-AGAGTT TGATCATGGCTCAG-3′) [77] and U1492R (5′-CGG TTACCTTGTTACGACTT-3′) [78]. The archaeal genes encoding 16S rRNAs were amplified using the Arc8 F forward primer (5′-TCCGGTTGATCCTGCC-3′) [79] and the Arc1492R reverse primer (5′-GGCTACCTTGTT ACGACTT-3′) [79]. The amplification program consisted of an initial denaturation step at 95 °C for three minutes, followed by 30 cycles consisting of one minute at 94 °C, 1 min of hybridization at 53 °C for bacterial DNA amplifications or at 50 °C for archaeal DNA amplifications and a two-minute elongation step at 72 °C. A final elongation at 72 °C was carried out for six minutes, after which the amplification products were stored at 12 °C. Sanger sequencing of the PCR products using forward and reverse primer was subcontracted to Genewiz (Leipzig, Germany). Contig assembly was then performed with Geneious v11.0.5. software, and similarity values to the nearest relative sequences were then calculated with EzTaxon-e [53]. A phylogenetic analysis of the 16S rRNA gene sequences of *Sulfurimonas* representatives was then

carried out. The 16S rRNA gene sequences of the cultivated strains were aligned with the closest MAGs encoding a 16S rRNA gene sequence and all cultivated species, using Muscle v.5.1 [61], and the alignment was trimmed manually on Geneious v11.0.5. Next, a phylogenetic reconstruction was performed using the PhyML (v3.0) algorithm [80], with the Kimura 80 correction, based on 1056 homologous nucleotides. The branch support was computed with 1000 bootstrap iterations.

Results and discussion

Mineralogical and geochemical characterization of the sulfur deposit and the surrounding area

The 1- to 2-m tall deposit had a cabbage-like structure with an outermost layer composed of a reddish to ochreous Fe-oxyhydroxide coating and a shiny black material (Supplementary Fig. S1), that turned out to be volcanic glass upon binocular observation (Fig. 1). The interior contained a lining of sulfur crystals and drips projected inwards. This unusual structure had a morphology resembling the small (m-size) spatter deposits encountered in the vicinity of volcano summit (J.-C. Komorowski, personal communication), which were composed of vesicular basanitic lavas that agglutinate during quenching. It also shared similarities with sulfur solfatara found onland and seafloor sulfur chimneys as those encountered at Northwest Eifuku volcano [81]. Here, the mixed assemblages of sulfur and glass suggested a formation during expulsion of immiscible liquid sulfur and magma droplets at the seafloor.

Petrographical examination suggested that the structure was composed of an assemblage of native sulfur and volcanic glass. The presence of native sulfur was confirmed by bulk XRD analysis showing 100% α-sulfur (S_8) (Table 1) and XRF, respectively. The absence of any igneous minerals, together with bulk XRF analysis showing SiO_2 (1.52 to 2.43 w%), TiO_2 (0.10 to 0.16 w%), and Al_2O_3 (0.48 to 0.67 w%) (Table 1) were consistent with the presence of volcanic glass, yielding with Fe/Al, Ti/Al ratios of about 1.5 (g/g) and 0.25 (g/g), respectively. These compositions were similar to basanitic lava recovered at Fani Maoré and characterized by Fe/Al = 1.24 ± 0.18 (g/g, 2 sd) and Ti/Al = 0.23 ± 0.02 (g/g, 2 sd) [14, 82].

Recovered fluid from the cracked open cavity (Fig. 1B) yielded similar chemical composition than background deep seawater for major cations (Na^+, Ca^{2+}, K^+, Mg^{2+}) and anions (Cl^-, SO_4^{2-}) (Table 2). Although the temperature probe was faulty at the time of sampling, the lack of shimmering effect produced when the arm of the ROV broke the cavity suggests that there was no temperature anomaly

Table 1 Mineralogy and geochemical composition determined by XRF (left) and XRD (right) of bulk samples from the Fani Maoré sulfur deposit, respectively

Analytes	Units	GFL_PL777_08_PBT02	GFL_PL781_12_PBT01	Analytes	Percentage	GFL_PL777_08_PBT02	GFL_PL781_12_PBT01
P.F 1050 °C	wt%	n.m	n.m	Alpha-sulfur	%	100	100
SiO_2	wt%	1.52	2.42				
TiO_2	wt%	0.10	0.16				
Al_2O_3	wt%	0.48	0.67				
Fe_2O_3	wt%	0.55	0.78				
MnO	wt%	0.005	0.01				
MgO	wt%	0.154	0.241				
CaO	wt%	0.255	0.360				
Na_2O	wt%						
K_2O	wt%	0.115	0.165				
P_2O_5	wt%	0.06	0.09				
S	wt%	59.5	78.8				
Total	wt%	61.22	81.28				
Co	µg/g	< 10	< 10				
Cr	µg/g	16	12				
Cu	µg/g	53	< 20				
Ni	µg/g	< 20	< 20				
Sr	µg/g	77	117				
Zn	µg/g	< 10	< 10				
Zr	µg/g	30	25				

Legend: *n.m.* not measured

Table 2 Environmental parameters of background seawater and fluid recovered from the sulfur deposit at Fani Maoré (Ti: titanium syringe, HY: seawater recovered from hydrocas)

Analytes	Units	GFL_PL781_12_TiD2	Reference background seawater*
pH		6.83	8.00
AT	mmol/l	2.83	2.41
H_2S	µM	< 0.1	< 0.1
Cl^-	mM	555.8	559.0
Br^-	mM	844.0	844.9
SO_4^{2-}	mM	29.0	29.1
Na^+	mM	476.1	478.1
K^+	mM	10.2	10.3
Mg^{2+}	mM	53.8	53.9
Ca^{2+}	mM	10.3	10.3
Si	µM	171	155.6
Fe	µM	2.19	< 0.05
Mn	µM	1.57	< 0.05
Li	µM	25.5	26.5
B	µM	423.6	462.0
Rb	µM	1.42	1.39
Sr	µM	96.3	92.4
U	nM	12.0	13.1
P	µM	2.5	3.4
Cu	nM	5.9	12.1

Legend: *Reference background seawater determined using (i) deep seawater recovered by CTD hydrocast (sample GFL_HY03_B01) at 2596 m depth for pH, AT and trace element composition determined by HR-ICP-MS (Si, Fe, Mn, Li, B, Rb, Sr, U, P, Cu); and (ii) deep seawater recovered in PBT-box (sample GFL_PL777_08_PBT01) at 2560 m depth for major element composition determined by IC (Cl^-, Br^-, SO_4^{2-}, Na^+, K^+, Mg^{2+}, Ca^{2+})

or active venting in the structure. However, a lower pH (6.83 vs 8.00) and higher alkalinity (2.83 *vs* 2.41 mmol.L^{-1}) in the fluid inside the structure compared to bottom seawater suggested a significant gas enrichment (e.g. CO_2, SO_2, and H_2S) in the chimney-like structure. In addition, native sulfur grains showed the release of significant amounts of H_2S and possibly SO_2 and CO_2 trapped as fluid inclusions inside the mineral, which could also be a source of acidity for the seawater trapped within the structure. As previously reported in volcanic systems, the formation of molten sulfur may occur through reaction (1) or (2).

(1) disproportionation of SO_2, producing also H_2S and H_2SO_4 [16, 83]

$$4SO_2(aq) + 4H_2O = H_2S(aq) + 3H_2SO_4(aq)$$

$$3SO_2(aq) + 2H_2O = S^0 + 2H_2SO_4(aq)$$

(2) synproportionation of SO_2 and H_2S [84]

$$SO_2(aq) + 2H_2S(aq) = 3S^0 + 2H_2O$$

Characterization of the geochemistry and mineralogy of this cavity in the Fani Maoré volcano has revealed the significant presence of sulfur compounds (notably S^0, SO_4^{2-}, and H_2S). Preliminary S-isotopes analyses of hand-picked native sulfur minerals yielded $\delta^{34}S$ values ranging from −0.07 to 0.66‰ (± 0.20 ‰, 2 sd), which was within the range of magmatic values [85, 86]. Sulfur isotope signatures therefore differed from those encountered for native sulfur deposits from seafloor hydrothermal systems which yield larger range, and often negative $\delta^{34}S$ values (e.g., [18]). It is therefore likely that native sulfur resulted from the synproportionation of magmatic SO_2 and H_2S [84] expelled during the eruptive event. Following its formation and rapid cooling at the seafloor, it is highly probable that chemosynthetic microbial communities were established in this micro-environment, deriving their energy from the transformation of these sulfur compounds via redox reactions. Microbial communities including notably sulfur-oxidizing *Bacteria* have already been observed in submarine volcanic ecosystems [87].

A potential chemosynthetic microbial diversity

Based on the seventy-one single-copy core genes present in bacterial genomes (detailed in Supplementary Table S1) [60], this sample would contain ninety-four bacterial genomes. This ecosystem was thus inhabited by diverse microbial taxa and dominated by *Bacteria* at the time of sampling. The total taxonomic diversity and relative microbial abundances in the bulk sample were studied by examining (i) the sequence diversity and relative abundance of the 16S rRNA genes sequences before read assembly, and (ii) that of the most abundant large ribosomal protein (L16) after read assembly (Fig. 2A). In addition to a low archaeal diversity (*Nanoarchaeota* phylum), both approaches indicated the presence of taxa belonging to eleven bacterial phyla, with the most abundant being *Bacteroidota* (representing 29.6 and 17.4% of total 16S rRNA genes sequences and L16 encoding sequences, respectively), *Campylobacterota* (24.6 and 60.0%), *Desulfobacterota* (13.6 and 3.6%) and *Pseudomonadota* (24.5 and 18.0%) (including *Alphaproteobacteria* (10.0 and 9.3%), *Gammaproteobacteria* (13.6 and 8.0%) and *Zetaproteobacteria* (< 1% in both cases)). Within these phyla, the families with the highest relative abundances (> 3%) based on 16S rRNA gene sequences, were *Flavobacteriaceae* (24.3%; *Bacteroidota*), *Sulfurimonadaceae* (14.4%; *Campylobacterota*), *Desulfocapsaceae* (9.1%; *Desulfobacterota*), *Rhodobacteraceae* (7.7%; *Pseudomonadota*), *Sulfurovaceae* (6.7%; *Campylobacterota*), *Geopsychrobacteraceae* (3.4%; *Desulfobacterota*), and *Sulfurospirillaceae* (3.3%; *Campylobacterota*), respectively.

Pseudomonadota (*Alphaproteobacteria* and *Gammaproteobacteria)* have been previously observed around newly formed submarine ridge volcanoes and are also present in the marine environment, while phyla such as *Campylobacterota* and *Desulfobacterota* are often associated with marine volcanic habitats [6, 88]. *Bacteroidota* are ubiquitous and frequently encountered in marine habitats [89].

Sequences from *Spirochaetota*, *Patescibacteria*, *Verrucomicrobiota*, *Planctomycetota* and *Bacillota* were much less abundant, each representing less than 4% of all sequences.

Genome-resolved metagenomics was also implemented and allowed the reconstruction of 23 bacterial MAGs, composed of 41 to 648 contigs (Supplementary Table S3). The 23 MAGs were affiliated to eight different microbial phyla (Fig. 2B), which represent around 62% of the microbial diversity at the phylum level in the natural sample, based on observed 16S rRNA gene sequences (Fig. 2A). No archaeal MAGs could be reconstructed. Based on quality criteria, 14 MAGs were of high quality (completion >90%; contamination <5% and at least 18 tRNAs) and nine MAGs were of medium quality (completion ≥50%; contamination <10%) (Supplementary Table S3) [90]. Seven MAGs were assigned to the phylum *Pseudomonadota*, six to *Bacteroidota*, three to *Campylobacterota*, followed by two assigned to *Desulfobacterota* and *Planctomycetota*, and one to *Verrucomicrobiota*, *Bacillota* and *Patescibacteria* (Fig. 2B).

The two MAGs *Planctomycetota*_MAG01 and *Patescibacteria*_MAG21 were derived from classes with no cultivated representatives. At genus and family level, there were nine and seven MAGs derived from taxa with no cultivated representatives, respectively (Supplementary Fig. S3). Twenty-two MAGs could be assigned up to the genus level with GTDB-Tk v2.4.0. Among them, *Desulfobacterota*_MAG05, *Desulfobacterota*_MAG12, *Campylobacterota*_MAG16, *Planctomycetota*_MAG17, and *Campylobacterota*_MAG22 belonged to the genera *Desulfuromusa*, *Desulfocicer*, *Sulfurimonas*, *Gimesia*, and *Sulfurovum*, respectively. The various closest bacterial relatives of these five MAGs assigned to a genus were known to grow by S^0 reduction (*Desulfuromusa kysingii*) [91, 92], H_2S, S^0 and/or $S_2O_3^{2-}$ oxidation (*Sulfurimonas* sp. and *Sulfurovum* sp.) [93, 94], SO_4^{2-} reduction (*Desulfocicer vacuolatum*) [95], and aerobic organoheterotrophy (*Gimesia* sp.), respectively [96]. Reconstruction of these first MAGs related to taxa involved in the microbial sulfur cycle was probably explained by the abundance of sulfur compounds (H_2S and S^0) in situ. Two other MAGs, *Pseudomonadota*_MAG08 and *Pseudomonadota*_MAG09, belonging to the families *Beggiatoaceae* and UBA6429 respectively, whose only genus with cultivated members is *Thiohalophilus*, could also derive from microorganisms with a dissimilatory metabolism involving sulfur species, as these families contain thioautotrophic and large sulfide-oxidizing *Bacteria,* respectively [70]. Various representatives of the phyla *Pseudomonadota* and *Bacteroidota,* which are highly represented in this environment, are also known to reduce S^0 [97]. For example, *Thioflexitrix psekupsensis*, *Beggiatoa leptomitoformis* and *Thiotrix nivea* which are taxonomically close to *Pseudomonadota*_MAG08 and *Pseudomonadota*_MAG09 notably, are sulfur-oxidizing bacteria [98–100].

Closest relative taxa corresponding to reconstructed MAGs were selected and their origin was indicated by colored dots in Fig. 2B (inner circle). MAGs reconstructed in this study were close to genomes/MAGs of taxa from various environments such as volcanoes, seawater, sediments, sulfur-rich habitats and redoxcline environments (e.g., deep-sea hydrothermal vents) [101–105] (Fig. 2B; Supplementary Fig. S2). Therefore, this microbial community partly resembled that of chemosynthetic marine environments, redoxcline habitats and seawater.

(See figure on next page.)

Fig. 2 **A** Taxonomic assignment and relative abundance of the sequences at the phylum level (*Bacillota*, *Planctomycetota*, *Verrucomicrobiota*, *Patescibacteria*, *Desulfobacterota, Campylobacterota, Bacteroidota*) or class level (*Alphaproteobacteria* and *Gammaproteobacteria* (both from the phylum *Pseudomonadota*) in the sulfur-rich sample of the Fani Maoré submarine volcano based on genes encoding the L16 ribosomal protein after read assembly (L16), based on 16S rRNA gene sequences before read assembly (16S), and within the reconstructed MAGs (MAG). For "16S", "Others" include *Bacteria* (*Spirochaetota* with a relative abundance of 0.026, *Bdellovibrionota* (0.025), *Fusobacteriota* (0.0011), *Myxococcota* (0.0008), *Pseudomonadota*: *Zetaproteobacteria class* (0.009)) and *Archaea* (*Nanoarcheota* (0.0008)) and other microbial sequences not assignated to a phylum (0.0254). For L16, "Others" include *Pseudomonadota: Zetaproteobacteria class* with a relative adundance of 0.007. **B** Maximum likelihood phylogenetic tree based on 71 single-copy core genes, constructed with FastTree implemented in Anvi'o, showing the position of the 23 MAGs from the Fani Maoré submarine volcano (in red) and close relatives (in black), indicating the taxonomic affiliation at the phylum level (outer circle), and the estimated optimal growth temperature (middle circle). The environment of origin of the closest relatives is symbolized by a colored dot. The optimal growth temperature of the taxa related to the MAG(s) was calculated using the TOME software and is represented in the form of a colored rectangle (middle circle). Optimal growth temperature ranging from 18 to >35 °C is represented by colors ranging from dark blue to red, respectively. This tree topology was confirmed by running the same alignment on IQ-TREE by maximum likelihood method, with 1000 iterations (Supplementary Fig. S2)

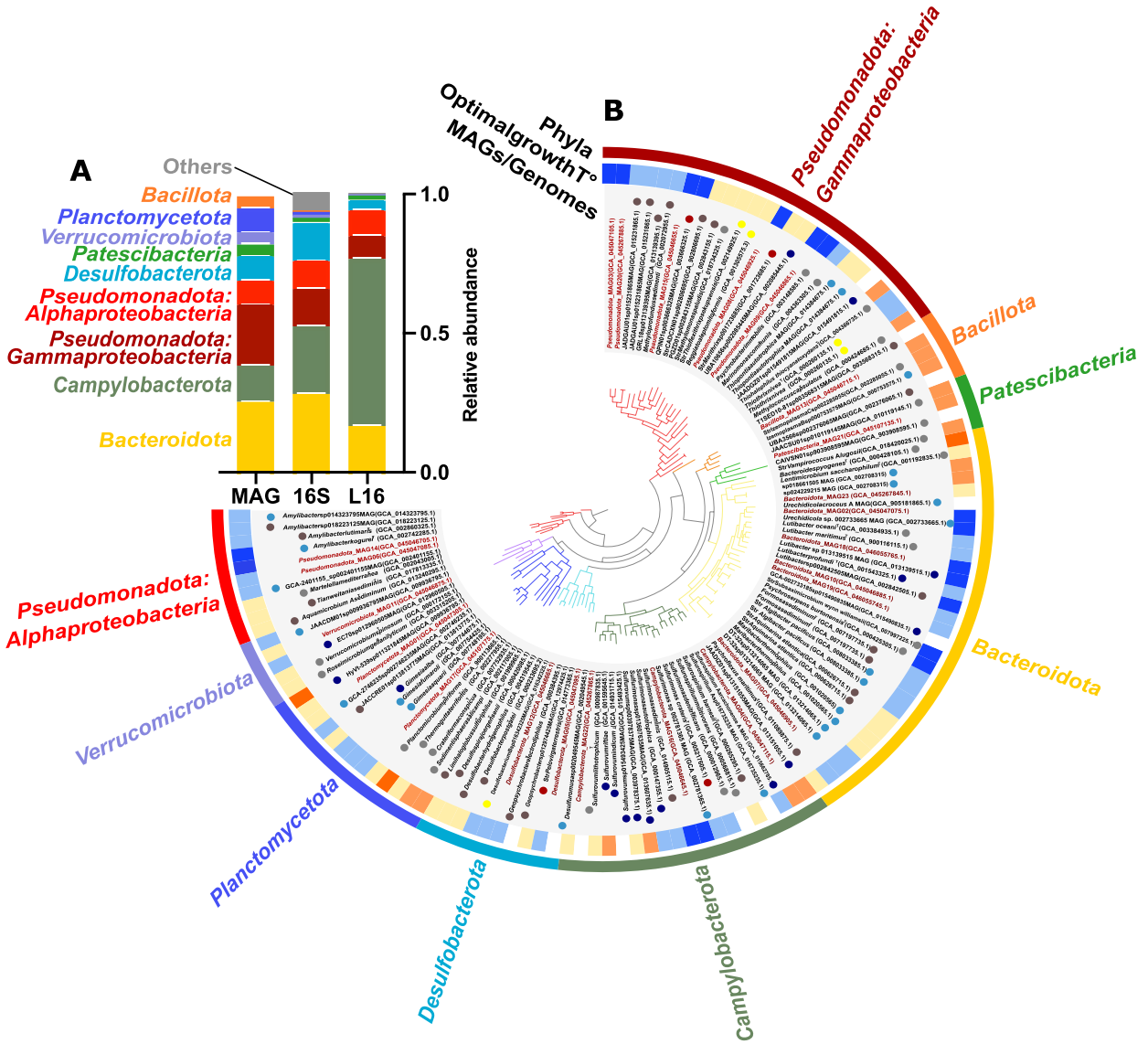

Fig. 2 (See legend on previous page.)

Interestingly, although this volcanic system differs greatly from active and inactive/low-temperature hydrothermal systems of the mid-ocean ridges, it is interesting to note that the microbial community of this submarine volcano studied only 3 years after eruption (and with no active venting at the time of sampling), encompassed both many phyla frequently found in active hydrothermal vent systems, such as *Campylobacterota*, and phyla found in hydrothermal vents whose activity decreased dramatically (collected ~ 7 years after the temperature of fluid emissions decreased significantly following a volcanic eruption), such as *Pseudomonadota* (*Gamma-* and *Alphaproteobacteria*), *Desulfobacterota*, and *Bacteroidota* [4].

Bacteria with a highly versatile physiology and metabolism were pesent, in particular members of

certain *Campylobacterota* genera. Within this phylum, the genera *Sulfurimonas* and *Sulfurovum* include members able to grow by oxidation of sulfur compounds using NO_3^- or O_2 as terminal electron acceptors, by reduction of S^0 and by disproportionation of S^0 or $S_2O_3^{2-}$ [93, 94, 106].

Notably, certain species of the genus *Sulfurovum* have been reported to be particularly efficient at exploiting solid S^0 [107]. *Sulfurimonas* taxa have also been shown to be highly competitive *Bacteria* for colonizing new habitats and to be widespread in various natural environments, including marine sediments, mangrove sediments, redoxcline habitats, oxygen minimum zones and deep-sea hydrothermal vents and plumes, and to predominate in the warm zones of marine hydrothermal vents [26, 70, 71, 106, 108]. They have also been reported to be among the main diazotrophs in mangrove sediments, dominating dark nitrogen fixation [109]. Among them, *Campylobacterota*_MAG16 represented a new species of *Sulfurimonas* (ANI value < 95%) not referenced in GTDB and most closely related to a MAG from Brothers volcano (referenced as Sulfurimonas_sp027047745 in GTDB), on the Kermadec volcanic arc (Fig. 3), which clustered mainly with taxa from hydrothermal vents and volcanic zones, including the ubiquitous taxon *Ca.* "Sulfurimonas pluma" [26, 27] and *Sulfurimonas autotrophica* [93].

The optimal growth temperatures predicted by the TOME software were between 18 and 33 °C (Fig. 2B, middle circle). This environment could therefore be mainly colonized by mesophilic microorganisms that may have migrated from deep-sea relay habitats (whale carcasses or submerged woods) for chemosynthetic microorganisms, from deep-sea distant hydrothermal vents, from subsurface sediments or cold seeps, or simply from background seawater where they may have persisted as seed banks (Fig. 3).

Versatile metabolic potentials

Presence of key enzymes and completion of metabolic pathways involved in carbon fixation, ATP synthesis, sugar metabolism, fatty acid metabolism, nitrogen metabolism, amino acid metabolism, hydrogen metabolism, iron metabolism, and sulfur metabolism were analyzed for the reconstructed MAGs (Figs. 4 and 5).

Firstly, regarding carbon fixation, based on the presence of key enzymes (detailed in Fig. 4 legend) from the six known natural carbon fixation pathways (the Calvin-Benson-Bassham cycle (CBB), the reductive tricarboxylic acid cycle (rTCA), the reductive acetyl-CoA (also called Wood-Ljungdahl (WL)) pathway, the 3-hydroxypropionate (3-HP) bicycle, the 3-hydroxypropionate/4-hydroxybutyrate (3-HP/4-HB) cycle and the dicarboxylate/4-hydroxybutyrate (DC/HB) cycle)) [110], results revealed that, with only three exceptions (*Pseudomonadota*_MAG15, *Verrucomicrobiota*_MAG11, and *Bacillota*_MAG13), all MAGs encoded one or more key enzymes of these carbon fixation pathways. This suggests that many taxa could grow autotrophically (Fig. 4). Carbohydrate degradation pathways (Embden-Meyerhof-Parnas, Entner-Doudoroff, and pentose-phosphate pathways) were also encoded in nine MAGs, and the fatty acid degradation pathway

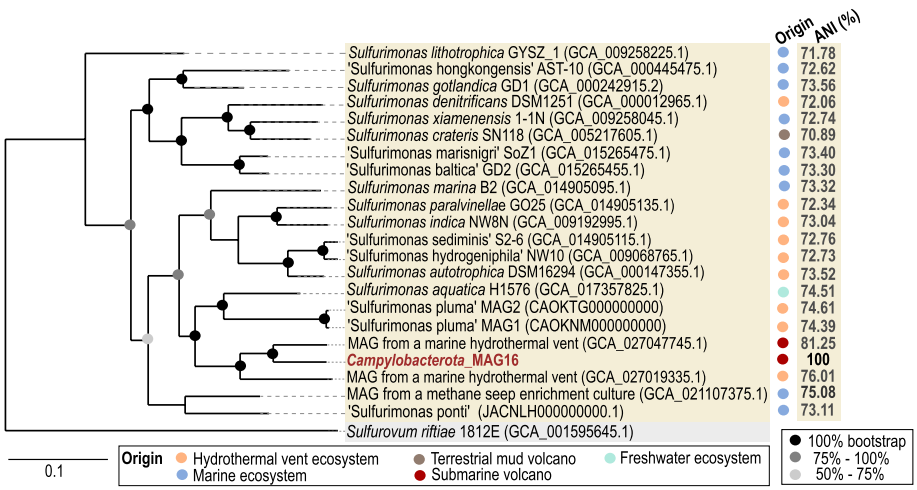

Fig. 3 Maximum-likelihood phylogenomic tree showing the phylogenomic position of MAG16 relative to *Sulfurimonas* species and closest MAGs, based on 250 concatenated single-copy gene clusters. The genome sequence of *Sulfurovum riftiae* was used as an outgroup. Bootstrap scores are shown at branch nodes by circles of different shades of grey. Bar, 0.1 amino-acid substitution rate. Colored dots on the right represent origin: orange: hydrothermal vent system, dark blue: marine ecosystem, light blue: freshwater ecosystem, dark red: submarine volcano and brown: terrestrial mud volcano. ANI values between *Campylobacterota*_MAG16 and other genomes of the genus *Sulfurimonas* are shown on the right

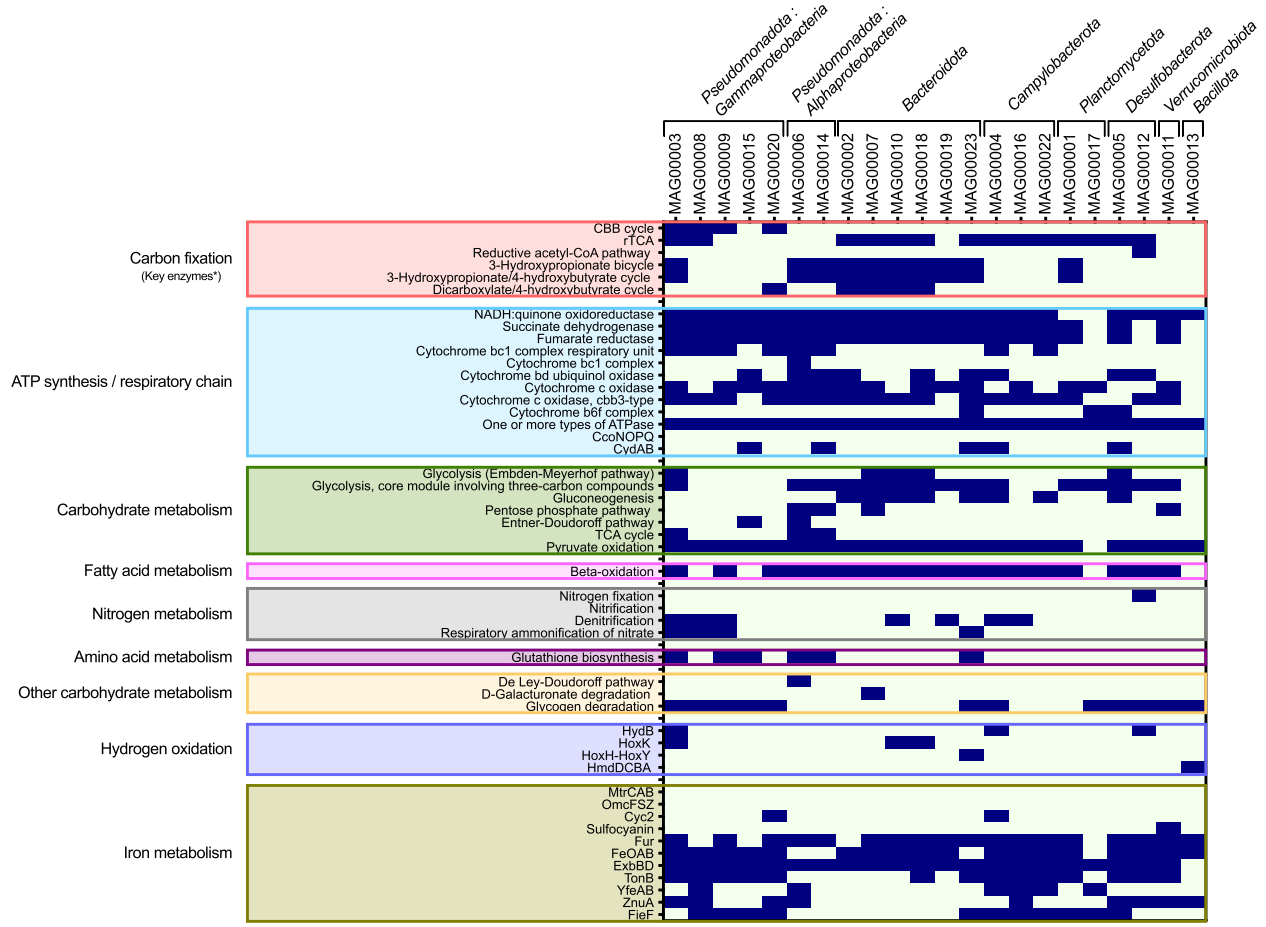

Fig. 4 Map illustrating the presence of complete metabolic pathways or the presence of a gene- or gene clusters-encoding proteins after gene prediction with Prokka, MaGe and Anvi'o, for 22 MAGs from the Fani Maoré submarine volcano. Genes involved in iron metabolism were predicted with FeGenie. *Patescibacteria*_MAG21 is not included because it does not code for any of these pathways/enzymes with the exception of the Fur enzyme. *The presence of carbon fixation pathways was based on the search for key enzymes for each pathway [110] and are indicated by a dark blue rectangle if key enzymes were present. For the CBB cycle, the key enzyme sought was the ribulose-1,5-bisphosphate carboxylase/oxygenase (RuBisCO), for the rTCA cycle, the key enzymes were 2-oxoglutarate synthase and isocitrate dehydrogenase, for the reductive acetyl-CoA pathway, the key enzymes were the NADP + dependent formate dehydrogenase, the carbon-monoxide dehydrogenase and the carbon-monoxide-methylating acetyl-CoA synthase, for the 3-HP, the key enzymes were the acetyl-CoA carboxylase and the propionyl-CoA carboxylase, for the 3-HP/4-HB, the key enzymes were the acetyl-CoA carboxylase and the propionyl-CoA carboxylase, and for the DC/4-HB, the key enzymes were the pyruvate synthase and the phosphoenolpyruvate carboxylase. For other metabolisms, the presence of complete pathways or the presence of genes clusters coding for the enzymes listed, are indicated by a dark blue rectangle

(beta-oxidation) in all but four MAGs (*Pseudomonadota*_MAG08, *Pseudomonadota*_MAG15, *Planctomycetota*_MAG17, and *Bacillota*_MAG13). Altogether, these results tend to indicate that most MAGs were from mixotrophic taxa, although it should be kept in mind that many enzymes in these pathways are reversible and could be used to synthesize amino acids, fatty acids or nucleic acids (Fig. 4).

The presence of pathways for organic carbon degradation could indicate that there was available organic carbon near the submarine volcano. This is in line with a recent study which showed that ocean waters located in the same province as the Fani Maoré volcano were rich in organic carbon, which could come from rivers in Mozambique and Madagascar [111]. The organic matter present in the deep waters and sediments could also have been resuspended by the violent volcanic eruptions of the Fani Maoré volcano. Alternatively, as typically observed in new chemosynthetic habitats, heterotrophic growth could be based on biomass or necromass synthesized by autotrophic microorganisms.

In total, 15 MAGs may have the ability to respire O_2, as they coded for aerobic respiration enzymes or for cytochromes optimized for microaerobic environments (*cbb3*-type cytochrome *c* oxidase; cytochrome *c* oxidase;

Fig. 5 Map showing the presence or absence of predicted microbial sulfur cycle genes/proteins based on Prokka, MaGe and Anvi'o annotations (and with DiSCo software for the genes *dsrABC*, *dsrMKJOP*, *dsrD*, *dsrEFH*, *dsrL*, *dsrT*, *hdrABC*, *qmoABC*, *sat*, *aprAB*, and *aprM*). The "ox." and "red." labels correspond to the flags given in the DiSCo output: ox. for oxidative; red. for reductive or disproportionation. The presence of the listed genes is indicated by a dark green cell

cytochrome *bd* ubiquinol oxidase) (Fig. 4). O_2, present in the surrounding seawater, was most likely available near the outer surface of the cavity and could be used as a terminal electron acceptor for respiration, notably coupled with oxidation of S^0 and H_2S present in situ.

As for *Campylobacterota*_MAG16, affiliated to the genus *Sulfurimonas*, it may be able to assimilate CO_2 with the rTCA cycle. This is consistent with the known ability of this taxon to fix carbon dioxide using the rTCA cycle [112]. Moreover, *Campylobacterota*_MAG16 encoded cytochrome *c* oxidase and *cbb3*-type cytochrome *c* oxidase, suggesting that it could reduce oxygen via *cbb3*-type cytochrome *c* oxidase under microaerobic conditions (< 20%; typically 2–10% dioxygen), and via cytochrome *c* oxidase under fully oxic conditions, coupled with sulfur oxidation [108].

Regarding iron metabolism, reconstructed MAGs did not code for any known iron reduction pathways,

but three of them did code for enzymes involved in iron oxidation. *Campylobacterota*_MAG04 and *Pseudomonadota*_MAG20 coded for *cyc*2 genes, belonging to *cyc*2 clusters 2 and 1, respectively, described elsewhere [113] (Supplementary Table S4; Fig. 4). *Verrucomicrobiota*_MAG11 encoded a sulfocyanin, an iron oxidase present in certain iron-oxidizing archaea [114]. The ability to produce energy through iron catabolism may be underestimated, as the iron catabolic pathways remain largely unknown [115]. In addition, several MAGs also encoded genes involved in iron transport (FeoAB, FutB, YfeAB, FbpABC), regulation of iron uptake (Fur, FecR), siderophore synthesis, siderophore transport (TonB-ExbB-ExbD, PirA, LbtU), and iron storage (ferritin) (Supplementary Table S4) [68].

Regarding nitrogen metabolism, three MAGs belonging to the phylum *Pseudomonadota*, two to *Campylobacterota*, and two to *Bacteroidota* encoded a full denitrification pathway.

The MAGs *Pseudomonadota*_MAG03, *Pseudomonadota*_MAG06, *Pseudomonadota*_MAG09, *Pseudomonadota*_MAG14, *Pseudomonadota*_MAG15, and *Bacteroidota*_MAG23, coded for a complete glutathione biosynthesis pathway. Glutathione has many functions, including improving the assimilation and oxidation of sulfur [116]. *Pseudomonadota* are known to own a large number of glutathione *S*-transferases in their genome [117]. A complete pathway for glutathione biosynthesis was encoded in some MAGs (Fig. 4) from sulfur-oxidizers like MAGs *Pseudomonadota*_MAG03, *Pseudomonadota*_MAG09 and *Pseudomonadota*_MAG15. However, for some MAG, such as *Campylobacterota*_MAG16 affiliated to *Sulfurimonas* sp., the glutathione biosynthesis pathway was not complete, as previously reported for this genus [112].

Eight MAGs encoding for hydrogenases were also identified (Fig. 4). Hydrogenases are metalloenzymes catalyzing the reversible oxidation of hydrogen; thus, they can be involved in hydrogen uptake coupled to the reduction of various terminal electron acceptors such as S^0 or NO_3^- for example, or in the release of H_2 to remove excess reduced equivalents from cellular metabolism (e.g., fermentation) [118]. This was consistent with the fact that during the volcanic eruption, large quantities of H_2 were released, allowing the colonization of the volcano by hydrogenotrophic microorganisms. Hydrogenotrophic organisms could then have been maintained thanks to the hydrogen produced by microbial fermentation or by switching to organotrophic growth for organisms that code for the enzymatic arsenal needed to oxidize organic compounds.

*Patescibacteria*_MAG21, did not code for any of the pathways/enzymes listed above (except Fur), but did code for numerous genes whose function is unknown. The phylum *Patescibacteria* is known for its small genome sizes and lack of genes encoding metabolic functions [119]. They probably depend on a host for their survival, with which they would establish symbiotic or parasitic interactions [120]. *Patescibacteria* have been observed in many environments, including terrestrial environments [121] and various marine environments such as deep-sea hydrothermal vents and submarine volcanoes [120]. Their presence in this sample suggested the possibility of symbiotic or parasitic microbial interactions in this submarine volcano.

A majority of the MAGs have the metabolic potential to use sulfur compounds

Enzymes of the microbial sulfur cycle were investigated in greater details, as there was a massive input of sulfur in this ecosystem. Indeed, the massif and cavity of the singular meter-size structure contained abundant mineralization of native sulfur on the Fani Maoré submarine volcano, including deposits of S^0, H_2S degassed by minerals and SO_4^{2-} from seawater, which could be used to fuel the chemosynthetic microbial communities.

A majority of the reconstructed MAGs (70%, $n = 23$) coded for many enzymes involved in the microbial sulfur cycle, suggesting that they came from taxa capable of metabolizing sulfur compounds (Fig. 5).

Most of the reconstructed MAGs encoded several enzymes for oxidation of inorganic sulfur compounds (ISC), in particular *Pseudomonadota*_MAG03, *Pseudomonadota*_MAG08, *Pseudomonadota*_MAG09, *Pseudomonadota*_MAG15 and *Pseudomonadota*_MAG20, and *Campylobacterota*_MAG16 (Fig. 5). They belonged, among others, to the family *Beggiatoaceae* (*Pseudomonadota*_MAG08), the genus *Sulfurimonas* (*Campylobacterota*_MAG16), and the family UBA6429 with no cultivated representatives (*Pseudomonadota*_MAG09). These results are consistent with the fact that sulfur oxidation abilities have been experimentally demonstrated or proposed for most of these lineages [93, 122, 123].

*Campylobacterota*_MAG16, for example, from the genus *Sulfurimonas*, coded for the Sqr system, Fcc subunits, and for a truncated Sox system. These bacteria may be able to oxidize sulfur compounds using the SQR-FCC-Sox-CDY_2Z_2 system, as previously shown for other strains of this genus (Fig. 5) [124].

*Campylobacterota*_MAG22, of the genus *Sulfurovum,* encoded a full S^0 oxidation pathway which, in this genus, is the truncated Sox-CDY_2Z_2 system [106], consistent with the ability to grow by sulfur oxidation demonstrated for this genus. Based on these results, in this habitat, the main phyla capable of using sulfur oxidation were probably *Campylobacterota* and *Pseudomonadota*.

In addition, few MAGs had the genetic potential to perform SO_4^{2-} reduction (Fig. 5). This is the case for *Desulfobacterota*_MAG12, which was 93% complete and closely related to *Desulfocicer vacuolatum*, and coded for Sat, AprA, DsrABC, DsrMKJOP, QmoABC but not for AprB, perhaps because this MAG was incomplete. The ability of *Desulfocicer vacuolatum* to reduce SO_4^{2-} has been demonstrated experimentally [125].

Although the ability to reduce S^0 is widely distributed among microbial diversity, it was somewhat more difficult to discriminate between genetic potential for sulfur reduction from sulfur oxidation or sulfate reduction, as only few enzymes involved in sulfur reduction are currently identified (HydDACB; ShyCBDA/SuDH; Npsr; SreABC), and in some taxonomic groups long known to reduce S^0, none of them are detected. With regard to sulfur reduction metabolism, it is worth noting the presence of *Campylobacterota*_MAG04 from the family *Sulfurospirillaceae*, which encoded HydDC. However, given the taxonomic distance separating it from its closest cultivated taxa, it is difficult to speculate on the potential ability of this bacterium to respire S^0.

It was also difficult to determine which MAGs had the genetic potential to perform sulfur disproportionation, because there are clearly several sulfur disproportionation pathways, parts of which are not yet identified, and some of these pathways share enzymes with other metabolisms of the sulfur cycle, such as sulfate reduction for example [126–128]. Some MAGs could be derived from strains that might be able to grow via this catabolism.

Organic sulfur compound (OSC) transformation is also a key component of the sulfur cycle as OSC represent the second most important pool of reduced sulfur molecules in marine sediments [70]. The hydrolysis of these molecules can release sulfate or sulfite in the environment, which can enter the microbial sulfur cycle (Supplementary Table S5) [70]. Genes encoding enzymes involved in the transformation of OSC (formylglycine-generating sulfatase enzyme, arylsulfo-hydrolase, sulfoacetaldehyde acetyltransferase, taurine dioxygenase and sulfatase-domain encoding genes) were searched. It was found that many MAGs of *Bacteroidota* (*Bacteroidota*_MAG07 and *Bacteroidota*_MAG23), *Verrucomicrobiota* (*Verrucomicrobiota*_MAG11) and *Planctomycetota* (*Planctomycetota*_MAG01 and *Planctomycetota*_MAG17) encoded such genes, sometimes in large numbers (Supplementary Table S5). It has been previously reported that genomes of members of these phyla encoded numerous sulfatase genes, and were therefore involved in the release of sulfate [70]. For example, the *Verrucomicrobiota*_MAG11 encoded for four formylglycine-generating enzyme genes, five arylsulfohydrolases genes and 107 sulfatase-domain encoding genes. One or two genes coding for enzymes involved in the release of sulfite (sulfoacetaldehyde acetyltransferase and taurine dioxygenase) were also encoded in *Pseudomonadota*_MAG03, *Pseudomonadota*_MAG06, *Pseudomonadota*_MAG08, *Pseudomonadota*_MAG09, *Pseudomonadota*_MAG14, and *Pseudomonadota*_MAG20, so all representatives of the phylum *Pseudomonadota*.

Sulfur oxidation, sulfur reduction, sulfate reduction, and sulfur disproportionation were prevalent catabolic pathways in culture

The abundance of cultivable microorganisms in the natural sample for the different metabolisms of the sulfur cycle was determined using a method derived from the most probable number (MPN) [73]. Serial dilutions to extinction were carried out at three temperatures (6 °C, 20 °C and 40 °C), with nine dilution series (five replicates and one non-inoculated control per series), for eight different culture conditions. These conditions included (i and ii) disproportionation with S^0 or with $S_2O_3^{2-}$ and SO_3^{2-}, (iii and iv) sulfate reduction with H_2 or acetate as an electron donor, (v and vi) sulfur oxidation with S^0 or H_2S as an electron donor, and (vii and viii) sulfur reduction with H_2 or amino acids as electron donors. By comparing the abundance of cultivable microorganisms with the total microbial cell density in the natural sample, it was possible to determine the percentage of cultivability for each metabolism (Fig. 6). An analytical control of the substrates/products of the reactions was also carried out to ensure that growth was due to the targeted catabolism. The dominant cultivable taxa in the latest dilutions were also identified by 16S rRNA gene sequencing. Results of these experiments are shown in Fig. 6 and Supplementary Table S6.

Microbial growth was observed for the four targeted metabolisms of the sulfur cycle and differences in the abundance of cultivable microorganisms were observed between these metabolisms. It is worth noting that the abundance of microorganisms was generally lower for the metabolisms with the lowest energy yields (Supplementary Table S7).

The highest cultivable abundances were observed under conditions of sulfur-oxidation and sulfur-reduction with CO_2 as the carbon source, with 47% of the microorganisms present in the natural sample being cultivable (Fig. 6). Growth was observed in incubations carried out under sulfur (S^0) or sulfide (H_2S) oxidation conditions at 6 and 20 °C, as indicated by the production of SO_4^{2-} and the consumption of NO_3^- under certain conditions (Supplementary Table S6). Given the abundance of cultivable microorganisms, the oxidation of sulfur compounds could be one of the main metabolisms of

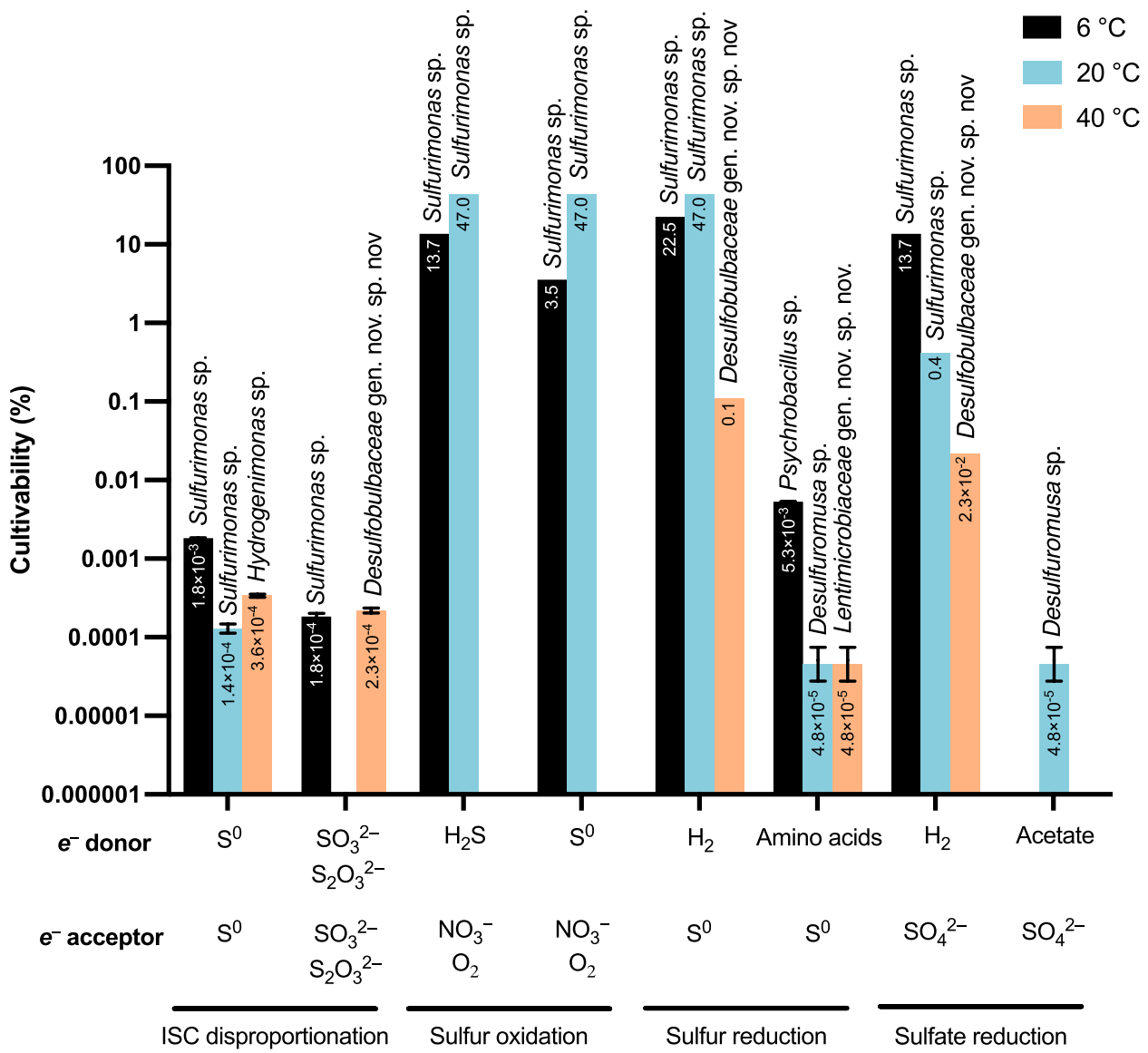

Fig. 6 Results of serial dilution for the different culture conditions and temperatures. The number in the bar charts indicates the percentage of cells in the cell community of the natural sample grown using this metabolism (e.g., 10^{-4} means that 0.0001% of microorganisms were able to grow by this metabolism at this temperature). The name above each bar chart is the closest cultured relative to the dominant species in the last dilution in which growth was obtained. Between the different temperatures, the difference in cultivable abundance was statistically significant only for the sulfur-oxidation metabolism (*p*-value 0.00279). ISC disproportionation: Inorganic Sulfur Compounds disproportionation

the sulfur cycle in this sulfur-rich deposit of the volcano (Fig. 6). Cultivable abundance of sulfur-oxidizing microorganisms (SOM) was significatively different between temperatures and no microbial growth was observed at 40 °C for any of these conditions (Fig. 6). High cultivable abundance of microorganisms for this metabolism was congruent with the large prevalence of S^0 in situ and the release of H_2S by the minerals near sulfur-rich deposits coupled to the presence of electron acceptors (e.g., O_2) in the surrounding seawater.

Similar cultivable abundance of microorganisms was also obtained in incubation targeting sulfur reduction, and growth was observed for the three incubation temperatures tested (6 °C, 20 °C, and 40 °C), when H_2 was used as the electron donor (Fig. 6). The growth was indeed attributable to the targeted catabolism, as H_2S was measured, indicating the reduction of S^0 (Supplementary Table S6). Under S^0 reduction conditions but with amino acids as electron donors and carbon sources, lower cultivable abundance was measured. However, at

40 °C, the absence of H_2S production and the formation of organic acids suggested that microorganisms did not grow by S^0 reduction under this condition, but by fermentation (Supplementary Table S6).

Up to 13.7% of the initial cell concentration in the natural sample was also cultivable in incubation targeting SO_4^{2-} reduction with H_2 as the electron donor (at 6 °C) and growth was also observed at 20 and 40 °C with lower abundance (Fig. 6). As with S^0 reduction, microorganisms able to use H_2 as an energy source were fairly abundant, consistent with the large quantities of H_2 released during the volcanic eruption [15]. However, a lower cultivable abundance was also obtained (only at 20 °C) when acetate was added as the electron donor and carbon source, and SO_4^{2-} as the terminal electron acceptor, which could be explain by the low energy yield of the reaction (Fig. 6).

Comparing the four catabolisms tested, the lowest cultivable abundances were observed under conditions of disproportionation of inorganic sulfur compounds. Microorganisms were able to grow under conditions of S^0 disproportionation or $S_2O_3^{2-}$ and SO_3^{2-} disproportionation. Under conditions of $S_2O_3^{2-}/SO_3^{2-}$ disproportionation, SO_4^{2-} and small amounts of H_2S were produced, and $S_2O_3^{2-}$ and SO_3^{2-} were consumed, confirming that microorganisms were able to grow by this catabolism. For S^0 disproportionation, small amounts of SO_4^{2-} and H_2S were produced, but it is not possible to assert that the strains grew via this metabolism, as S^0 consumption was not monitored. However, since the cultivation of sulfur-disproportionating microorganisms is favored if H_2S is removed by means of iron (III) hydroxide chelators [126] or by continuous sparging with N_2, which was not done in this study (in order to provide the same conditions in all experiments), it is possible that the actual abundance of sulfur-disproportionating microorganisms has been underestimated. Nevertheless, the disproportionation of sulfur compounds, although exergonic under the in situ conditions of various natural habitats [129, 130], remains a less energetic and therefore less favorable reaction overall than the other metabolisms of the sulfur cycling [131], and is probably not predominant at this site.

When examining the taxonomy of cultured microorganisms, some taxa present in the natural sample and identified by molecular approaches were not observed in culture. This is the case of *Planctomycetota*, *Patescibacteria*, and *Verrucomicrobiota*, which did not code for the catabolic pathways of the sulfur cycle and were obviously involved in other cycles. *Pseudomonadota* encoding sulfide oxidation pathways, on the other hand, were not dominant in cultures targeting sulfur/sulfide oxidation, suggesting either (i) that their in situ abundance was lower than that of other sulfide-oxidizing taxa (*Sulfurimonas* for example) or, (ii) that *Pseudomonadota* were slow growing bacteria (K-strategists) that were outcompeted by metabolically versatile bacteria with fast growth rates (R-strategists).

Campylobacterota were predominant taxa in culture

According to the sequencing results of the highest dilutions in culture, *Bacteria* belonging to the *Campylobacterota* phylum (in particular those of the genus *Sulfurimonas*) were predominant in cultures in terms of abundance and were grown by all four sulfur metabolisms tested (Fig. 6).

In sulfur oxidation conditions with H_2S or S^0 as the electron donor, at temperatures of 6 °C and 20 °C, the microorganisms grown in the latest dilutions were taxonomically close to *Sulfurimonas autotrophica*, a chemolithotrophic bacterium whose ability to oxidize S^0 and H_2S has been demonstrated in vitro [93]. These observations were also consistent with the genetic potential predicted for *Campylobacterota*_MAG16, which was also closely related to *Sulfurimonas autotrophica* (ANI score: 73.52%) and encoded a complete sulfur oxidation pathway (Fig. 5).

In the culture targeting S^0 reduction, identification of growing species also indicated the presence of strains closely related to *Sulfurimonas autotrophica* (with 98.10% 16S rRNA gene sequence similarity) at 6 °C and 20 °C, a species not reported to use sulfur reduction to grow, but which belongs to a genus encompassing other sulfur-reducing species [132, 133].

In S^0 disproportionation condition, taxonomic affiliation indicated the presence of two strains of *Sulfurimonas* at 6 °C and 20 °C and one *Hydrogenimonas* strain at 40 °C. Some *Sulfurimonas* species have been identified as capable of disproportionating sulfur [134], however, the 2 closest species (*S. autotrophica* and *S. paralvinellae*) have not been identified as such. *Hydrogenimonas thermophila* which is the closest relative of a strain grown under S^0 disproportionation conditions, grows anaerobically by using H_2 and S^0 as energy sources, and is known to grow by sulfur reduction, but not by sulfur disproportionation [135].

Overall, *Sulfurimonas* taxa were predominant microorganisms under six different autotrophic catabolic conditions at 6 °C and 20 °C, accounting for around 47% of the microbial cell concentration of the natural sample, suggesting that these taxa were probably abundant in situ. This result is congruent with the fact that *Sulfurimonadaceae* represented 14.4% of 16S rRNA gene sequences in metagenome dataset before read assembly. These *Sulfurimonas* strains were phylogenetically very close to each other (Fig. 7). Eight of them shared the same 16S rRNA gene sequence (Fig. 7). They belonged to the same sequence cluster as *Campylobacterota*_MAG_16

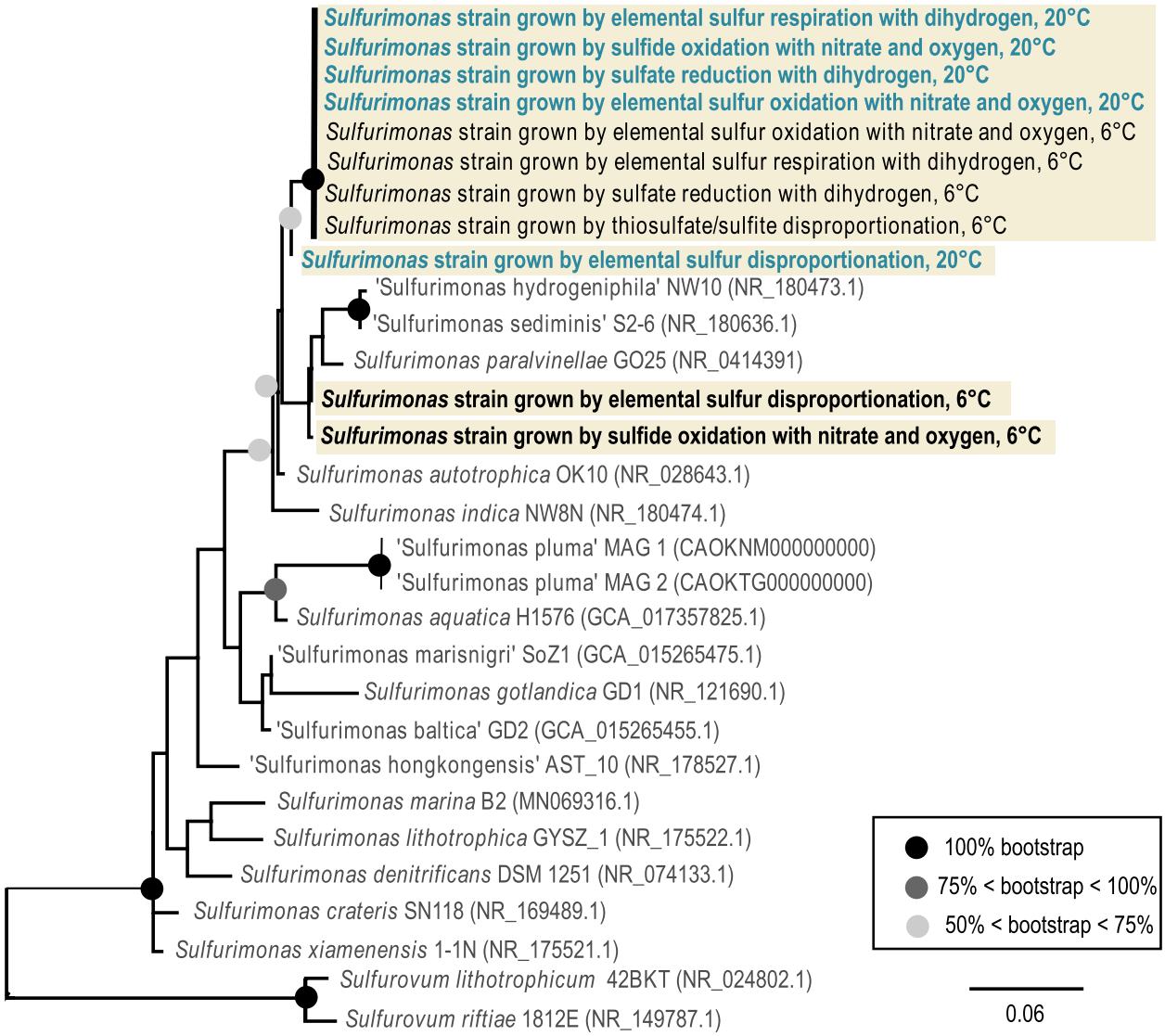

Fig. 7 Maximum likelihood tree showing the phylogenetic positions of the *Sulfurimonas* strains grown in the latest culture dilutions (highlighted in beige) and representatives of the genus *Sulfurimonas* (cultivated species and MAGs including a 16S rRNA gene), based on the 16S rRNA genes sequences (1056 nucleotide positions). Bootstrap values (expressed as percentages of 1000 replications) are shown at branch nodes. Bar, 0.06 nucleotide substitutions

(which does not encode a 16S rRNA gene sequence) (Fig. 3). Their genetic proximity added to the fact that the metagenome sequencing depth deployed here could have been greater may explain why only one *Sulfurimonas* MAG, *Campylobacterota*_MAG_16, has been reconstructed using metagenomics.

The finding that these strains were grown under six different metabolic conditions and at two different temperatures is consistent with the fact that the *Sulfurimonas* genus is known for its metabolic versatility, O_2 tolerance and involvement in sulfur metabolisms [108]. Moreover, the genus *Sulfurimonas* appears to be responsible for a large chemoautotrophic activity in different aquatic environments [108, 136], and a previous study showed the dominance of this genus in a volcanic ecosystem [3]. This genus is also ubiquitous in non-buoyant hydrothermal plumes and includes taxa (*Ca.* 'S. pluma') that have acquired genes enabling growth in oxygen-saturated pelagic environments, which have been proposed to be part of the oceanic microbial seed bank supporting dispersal and connection between pelagic and seabed/subsurface habitats via seawater [26].

Desulfobacterota, *Bacteroidota*, and *Bacillota* also showed a high culturability

Bacteria belonging to the *Desulfobacterota* phylum were also cultivated from the natural sample and observed in different culture conditions (S^0 reduction, $S_2O_3^{2-}$/SO_3^{2-} disproportionation, SO_4^{2-} reduction). Under S^0 reduction conditions with H_2 as the electron donor, a strain representing a putative new genus close to *Desulfobulbus alkaliphilus* (92.90% 16S rRNA gene sequence similarity) grew at 40 °C [137]. Under $S_2O_3^{2-}$ disproportionation conditions, the presence of a strain distantly related to *Desulfobulbus alkaliphilus* (93.19% 16S rRNA gene sequence similarity) grew in the latest dilutions, but this sulfate-reducing species is not known to use this catabolism to grow. However, it has already been shown that some *Desulfobulbus* species grow by anaerobic disproportionation of SO_3^{2-} and S^0 [126, 138]. Under conditions of S^0 reduction with amino acids as electron donors and carbon sources, at 20 °C, a production of H_2S and acetate was observed, and sequencing results indicated the presence of two species belonging to the genus *Desulfuromusa,* close to *D. succinoxidans* and *D. kysingii* (98.88 to 99.30% 16S rRNA gene sequence similarity). The latter are known to use sulfur reduction, under anaerobic mesophilic and anaerobic conditions with S^0 as electron acceptor. *D. kysingii* is also known to use amino acids as electron donors [92]. A strain close to *D. kysingii* (98.48% 16S rRNA gene sequence similarity) was also cultivated at 20 °C under SO_4^{2-} reduction conditions with acetate as an electron donor and a carbon source, but it is not possible to confirm that it grew by using this metabolism because no sulfate consumption was observed. Under SO_4^{2-} reduction conditions with H_2 as an electron donor at 40 °C, a representative of a new genus of *Bacteria* close to *Desulfolithobacter dissulfuricans* (93.74% 16S rRNA gene sequence similarity) was also cultivated. *Desulfolithobacter* species have already been isolated from marine hydrothermal vent ecosystems [139].

Bacteria of the *Bacillota* phylum were grown under the condition of S^0 reduction with amino acids as electron donors and carbon sources. At 6 °C, a bacterium close to *Psychrobacillus faecigallinarum* (99.48% 16S rRNA gene sequence similarity) was identified, and H_2S production was measured in this culture, suggesting that S^0 reduction was at work.

A representative of the *Bacteroidota* phylum grew under S^0 reduction conditions at 40 °C but no H_2S production was detected, while acetate production was measured. This strain identified in culture, which is distantly related to *Lentimicrobium saccharophilum* (89.36% 16S rRNA gene sequence similarity), may have developed via the Stickland reaction, which is a reaction based on two amino acids used as electron donor and electron acceptor, and which produces organic acids [140].

Autotrophic and heterotrophic carbon fixation could occur at Fani Maoré submarine volcano

In cultures, efficient growth was observed under autotrophic and heterotrophic conditions with either CO_2, amino acids or acetate as carbon sources, showing that both autotrophic and heterotrophic or mixotrophic microorganisms were present in this ecosystem, in line with the genetic potential of MAGs (Fig. 6). As mentioned above, most MAGs encoded key enzymes of known carbon fixation pathways (Fig. 4). Nor can we rule out the possibility that new carbon fixation pathways or variants of known pathways were encoded in these MAGs. For example an autotrophic carbon fixation pathway that cannot be predicted from metagenomic analyses alone was not included in our investigations, which if present, would potentially increase the importance of autotrophy in microorganisms in this environment. This is a variant of the rTCA cycle, known as the reverse oxidative tricarboxylic acid (roTCA) cycle, which could be expressed in some MAGs (e.g., *Desulfobacterota*_MAG05 and *Desulfobacterota*_MAG12) [141, 142]. Compared with rTCA cycle, this pathway lacks ATP-citrate lyase and requires abnormally high expression of citrate synthase to replace it.

Microbial growth was observed under both heterotrophic and autotrophic conditions at all three temperatures. Based on the maximum cultivable abundance measured, autotrophic microorganisms were about 10^4 more abundant than heterotrophic microorganisms (Fig. 6). Although not all microorganisms were cultivable here, these results suggest that this environment would be colonized mainly by autotrophic microorganisms, including representatives of the genus *Sulfurimonas*, which were predominant under eleven different combinations of metabolism and temperature.

Conceptual model of microorganisms/geosphere interaction in the Fani Maoré submarine volcano

Geological observations and geochemical analyses indicated that the sulfur deposit was intrinsically associated with volcanic activity and eruptive event. The latter has produced a significant amount of CO_2, methane (CH_4), H_2 [15] and probably sulfur dioxide (SO_2) and H_2S, which were released into the water column. H_2S was still being degassed by minerals. Large amounts of S^0 were also clearly visible in the vicinity of the sulfur deposit, in the form of small droplets and drips that suggest fallout of liquid sulfur that was quenched as it mixed with seawater. As the volcano was located in a marine environment, seawater SO_4^{2-} was also present in the surrounding waters. All these elements could be used by microorganisms in their metabolism. The biosphere-geosphere interactions likely to occur in this environment can be represented

in the form of a conceptual interaction model described below, based on environmental data, cultivation data and genomic potential of the main taxa (Fig. 8).

This environment could likely be subdivided into 3 areas as a function of the redox state of sulfur and the availability of O_2. The walls of the sulfur deposit and inside the cavity, where minerals continued to outgas H_2S, were probably anoxic, although fluid sampling did not identify such conditions due to rapid entrainment of surrounding seawater. Significantly lower pH in the fluid inside the cavity relative to seawater was however consistent with on-going oxidation of S^0 or SO_2 hydrolysis. The temperature inside the closed cavity may have been higher than that of seawater, at least in the initial stages of deposit formation and cooling. In the immediate outer layer of the deposit, where there was no longer any influence from gases (e.g., H_2S) and acidity emitted by degassing minerals and mineral dissolution, environmental conditions were most likely oxic and similar to background seawater, as confirmed by the extensive occurrence of Fe-oxyhydroxide covering the deposit. At the interface between these two zones was probably an Oxic Anoxic Transition Zone (OATZ), where a gradient of oxygen and chemical species would be established at the interface between the surface minerals and seawater.

Metagenomic analysis indicated that a majority of the taxa present in this habitat had the genetic potential to participate in one or more reactions of the microbial sulfur cycle and cultivation analyses demonstrated that strains can express one or more sulfur metabolisms, thus covering all reactions of the microbial sulfur cycle of all oxidation states (Fig. 8).

Representatives of three phyla could develop in the anoxic zone, in the walls of the sulfur deposit and inside the cavity, close to sulfide-degassing minerals given the metabolisms expressed in culture and the genetic potential of MAGs (Fig. 8). This was the case for *Desulfobacterota* representatives, as *Desulfobulbaceae* members were shown to be able to grow at 40 °C by anaerobic $S_2O_3^{2-}$ disproportionation and by SO_4^{2-} reduction. In addition, *Desulfuromusa* representatives were shown to grow by sulfur or sulfate reduction. These anaerobic microorganisms would likely be mainly responsible for the reductive reactions of the microbial sulfur cycle. Indeed, SO_4^{2-} reduction, S^0 reduction, and anaerobic sulfur disproportionation are three metabolisms known to occur under anaerobic conditions.

Then, in the OATZ, at the interface between the anoxic zone and the oxic zone, certainly on the outer

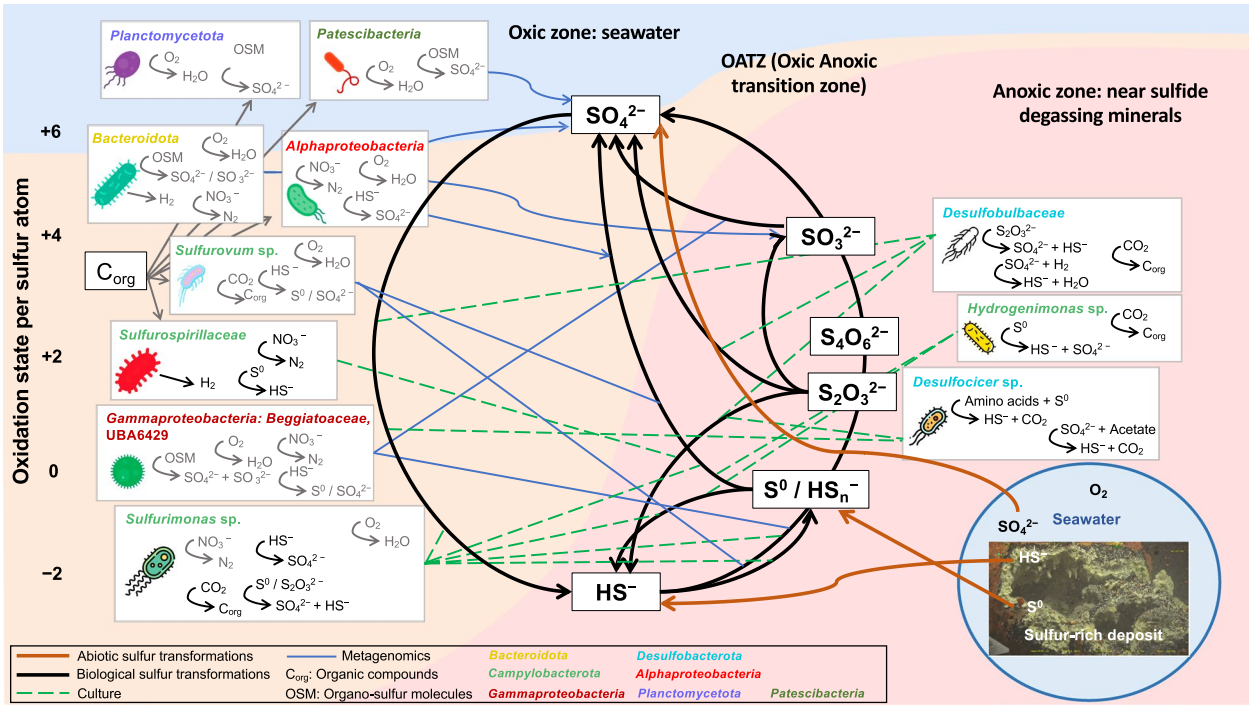

Fig. 8 Conceptual model of microorganisms/geosphere interactions at the Fani Maoré submarine volcano. This diagram summarizes the metabolisms expressed in culture (green dashed lines) and the metabolic genetic potential determined by metagenomic approach (solid blues lines). Biological transformations of sulfur and abiotic sources of sulfur are indicated by solid black and brown lines respectively. The form of this diagram is inspired by a graph published elsewhere [71]. Legend: OSM stands for Organic Sulfur Compounds

surface of the cavity walls, sulfur oxidation was likely to be prevalent. Indeed, sulfur/sulfide oxidizers could grow either in oxic or anoxic conditions, with H_2S oxidation occurring at a higher rate under oxic conditions than under anoxic ones. Under anoxic conditions, NO_3^- could be used as an electron acceptor instead of O_2. Several representatives of *Campylobacterota* are known to grow via this catabolism, such as *Sulfurimonas* species which were prevalent in cultures. The genus *Sulfurovum* is also known to use this catabolism under microaerophilic conditions. Cultivable microbial cell numbers were high at 6 °C and 20 °C in MPN incubations targeting S^0 and H_2S oxidation, which likely corresponded to temperatures encountered in the OATZ. Several MAGs affiliated to the *Pseudomonadota* could also be involved in sulfur oxidation and operate in this transition zone, such as the MAGs of the families *Beggiatoaceae* and UBA6429, which encoded several sulfur oxidation genes of the Sox system. Representatives of the phylum *Alphaproteobacteria* might also be involved in sulfur catabolism, especially in sulfur oxidation. Inorganic sulfur compound disproportionators could also be found in this zone. Some facultative anaerobic microorganisms could also be indirectly involved in the sulfur cycle, such as *Bacteroidota* that mediate transformations of organo-sulfur compounds, releasing SO_4^{2-} or SO_3^{2-} in the environment, which could then be used by other microorganisms.

Finally, in the oxic zone, a diversity of microorganisms could be found, some of them being involved in the sulfur cycle. They would include sulfur oxidizing *Bacteria* that were also found in the OATZ, represented by the class *Gammaproteobacteria* and the families *Beggiatoaceae* and UBA6429. *Campylobacterota* of the family *Sulfurospirillaceae* known to grow by S^0 reduction under microaerophilic conditions could also grow in this area [143]. This oxic zone would also be favorable for the growth of aerobic heterotrophs such as *Bacteroidota* or *Planctomycetota,* which have the ability to transform organosulfur compounds and release SO_3^{2-} and SO_4^{2-}, and also to produce H_2 to sustain hydrogenotrophs.

Conclusion

The Fani Maoré submarine volcano hosted a diversity of microorganisms using organic and inorganic carbon sources and a wide array electron donors and electron acceptors. Due to the abundance of sulfur compounds in the habitat, the study was focused on the microbial sulfur cycle. From the metagenomic approach, 23 MAGs belonging to 8 different phyla could be reconstructed. Most of them were affiliated with *Pseudomonadota*, *Bacteroidota*, and *Campylobacterota*. The large majority of the MAGs were derived from *Bacteria* involved in the sulfur cycle, especially in sulfur oxidation. The cultivable fraction of microorganisms shown by the culture-based approach derived from the MPN method highlighted a diversity of sulfur metabolisms, with high cultivation rates for sulfur reduction, sulfate reduction with dihydrogen, and sulfur oxidation. The identification of the dominant strains in each culture condition indicated the prevalence of strains belonging to the genus *Sulfurimonas*, under various autotrophic metabolic conditions. Their metabolic versatility may explain why they were prevalent. Culture-based experiments also showed that there were in situ microorganisms capable of producing energy from one or more sulfur-based metabolisms, giving ultimately a complete sulfur cycle. Only 3 years after the volcanic eruption this work demonstrated that the microorganisms identified in this intraplate sulfur-rich massif of the submarine volcano Fani Maoré, some of which are metabolically versatile, have the genetic and functional potential to drive a complete sulfur cycle, including reactions of oxidation, disproportionation and reduction of sulfur compounds. The Fani Maoré volcano represents a new example of a redoxcline habitat where the genus *Sulfurimonas* is fairly abundant. In the future, it would be interesting to investigate the genetic basis of the ecological success of the *Sulfurimonas* taxa and the reservoirs that enable them to colonize marine transient, neo-formed or changing habitats.

Supplementary Information

The online version contains supplementary material available at https://doi.org/10.1186/s40168-025-02153-3.

Additional file 1: Supplementary Table S1. List of the seventy-one single copy core genes used for MAG phylogenomic analysis on MAGs and for estimating Bacteria diversity. Additional file 2: Supplementary Table S2. List of the two hundred and fifty gene clusters used for the 14 phylogenomic analysis of *Sulfurimonas*. Additional file 3: Supplementary Figure S1. Photograph of the sulfur-rich closed cavity of the Fani Maoré before sampling. Videos of the sampling can be viewed by clicking on this link : https://video.ifremer.fr/video?id=46680. Additional file 4: Supplementary Figure S2. Maximum-likelihood phylogenomic tree based on 71 concatenated single copy core genes, showing the position of the 23 MAGs from the Fani Maoré submarine volcano (in red) and close relatives (in black), indicating the taxonomic affiliation at the phylum level. The tree was built by maximum-likelihood using IQ-TREE. Branch support, shown on the tree by circles in different shades of green, was computed with the aLTR SH-like method. The scale bar represents the expected number of changes per nucleotide position. Additional file 5: Supplementary Table S3. General characteristics of the 23 MAGs reconstructed from the sulfur-rich deposit at the top of the volcano. Legend: Completion and redundancy values were obtained with CheckM v2 implemented on the MaGe platform using lineage specific gene markers. The classification was determined with the classify workflow of the Genome Taxonomy Database GTDB-Tk v2.4.0. NB: In addition to the taxonomic affiliations at phylum, family and genus level, the taxonomic affiliation at class level is given for the MAGs belonging to the phylum *Pseudomonadota*. Additional file 6: Supplementary Table S4. Summary of iron-related genes or genes involved in iron metabolism

in reconstructed MAGs, based on FeGenie HMM profile search. (https://github.com/Arkadiy-Garber/FeGenie). Additional file 7: Supplementary Table S5. Table showing the number of enzymes involved in the transformation of organic sulfur compounds encoded in the reconstructed MAGs. The sulfur compound released by the transformation of these compounds is given in the second line of the table. MAGs with no enzyme hits were not included in this table. FGly-sulfatase: formylglycine-generating sulfatase enzyme. Additional file 8: Supplementary Table S6. Results of 16S rRNA gene sequence analysis and major variation of catabolic products identified by analytical methods. For ion species: +: increase (production); −: decrease (consumption). For H_2S: +: H_2S production; +/−: low H_2S production; −: no H_2S production. For $S_2O_3^{2-}$ disproportionation at 40°C, S^0 disproportionation at 40°C, S^0 reduction with H_2 at 40°C, S^0 reduction with amino acids at 40°C and SO_4^{2-} reduction with H_2 at 40°C, the bests hits are an uncultured species with the following accessions numbers: FJ264759 (97.65% 16S rRNA gene sequence similarity), AF367486 (98.29%), FJ264759 (95.95%), FJ497327 (98.15%) and FJ264759 (97.70%). Additional file 9: Supplementary Table S7. Examples of catabolic reactions of oxidation, reduction and disproportionation of sulfur compounds and biological standard free changes of these reactions. Standard Gibbs free energies are expressed for 298.15 K, 1 atm, pH 7 and 1 M of each chemical species (albeit proton).

Acknowledgements
We thank the cruise chiefs scientists of GEOFLAMME (E. Rinnert, C. Cathalot and N. Feuillet) and the captain and crew of R/V Pourquoi pas?, and ROV Victor 6000 for their logistical support for collecting samples. We thank Anne-Sophie Alix for help with producing Fig.1.A. We thank Hugo Doré and Léna Ailliot for their help in solving bioformatics problems, and Eva Pouder and Ludivine Michaudet for their support with FeGenie analyses. The LABGeM (CEA/Genoscope & CNRS UMR8030), the France Génomique and French Bioinformatics Institute national infrastructures (funded as part of Investissement d'Avenir program managed by Agence Nationale pour la Recherche, contracts ANR-10-INBS-09 and ANR-11-INBS-0013) are acknowledged for support within the MicroScope annotation platform. We thank four anonymous referees for their constructive comments.

Authors' contributions
KA and SY designed and managed the project. SY and MLM performed laboratory assays and data analysis and interpreted the data. OR, CC, ER, XP, AB, SC, VG and YG performed laboratory assays. JA, BT and KA performed data analyses. OR, ER, AG and EGR performed or supervised geochemical analyses. EGR supervised chemical analyses on cultures. OR, ER, AG and EGR collected samples and carried out on-board conditioning and analysis. KA interpreted the data and wrote the manuscript. SY, MLM, EGR and OR edited and wrote sections of the manuscript. All authors contributed to revisions of the manuscript, tables, and figures and approved the submitted version.

Funding
This work was funded by the CNRS-INEE as part of the Sino-French IRP 1211 MicrobSea to K.A., and by the French National Research Agency for the project MISD (with the Pole Mer Bretagne Atlantique label) under the reference ANR-22-CE02-0001 to K.A. The study was supported by a grant from the French Ministry of Higher Education and Research (UBO EDSML), and from the Région Bretagne, to S.Y. This research was supported by the Mayotte volcanological and seismological monitoring network (REVOSIMA, doi: 10.18715/MAYOTTE.REVOSIMA), by the French Oceanographic Fleet, by TotalEnergies (TOTAL ENERGIES FR000063751//876 IFREMER.
20/1001730) and by ISblue project, Interdisciplinary graduate school for the blue planet (ANR-17-EURE-0015) and co-funded by a grant from the French government under the program "Investissements d'Avenir" embedded in France 2030.

Data availability
This Whole Genome Shotgun project has been deposited at DDBJ/ENA/GenBank under the BioProject PRJNA938062, and accession numbers GCA_045047305.1, GCA_045047075.1, GCA_045047105.1, GCA_045047115.1, GCA_045047095.1, GCA_045047085.1, GCA_045046905.1, GCA_045046925.1, GCA_045046865.1, GCA_045046885.1, GCA_045046875.1, GCA_045046665.1, GCA_045046715.1, GCA_045046705.1, GCA_045046655.1, GCA_045046645.1, GCA_045107175.1, GCA_046055765.1, GCA_046055745.1, GCA_045267885.1, GCA_045107135.1, GCA_045267865.1 and GCA_045267845.1. 16S rRNA gene sequences of taxa cultivated by the approach derived from the most probable number method have been deposited at GenBank under the accession numbers PQ541048 to PQ541067. *Sulfurimonas* strains isolated in this study are stored at −80 °C with 5% (v/v) dimethylsulfoxide.

Declarations

Ethics approval and consent to participate
Not applicable.

Consent for publication
Not applicable.

Competing interests
The authors declare no competing interests.

Author details
[1]Univ Brest, CNRS, Ifremer, EMR 6002 BIOMEX, IRP 1211 MicrobSea, Unité Biologie Et Ecologie Des Ecosystèmes Marins Profonds BEEP, Plouzané 29280, France. [2]Geo-Ocean, UMR 6538 Ifremer, Université de Bretagne Occidentale, CNRS, Plouzané F-29280, France.

Received: 22 October 2024 Accepted: 28 May 2025
Published online: 15 July 2025

References

1. White SM, Crisp JA, Spera FJ. Long-term volumetric eruption rates and magma budgets. Geochem Geophys Geosyst. 2006;7(3):2005GC001002. https://doi.org/10.1029/2005GC001002.
2. Butterfield D, Nakamura K, Takano B, et al. High SO_2 flux, sulfur accumulation, and gas fractionation at an erupting submarine volcano. Geology. 2011;39:803–6. https://doi.org/10.1130/G31901.1.
3. Danovaro R, Canals M, Tangherlini M, et al. A submarine volcanic eruption leads to a novel microbial habitat. Nat Ecol Evol. 2017;1(6):144. https://doi.org/10.1038/s41559-017-0144.
4. Hou J, Sievert SM, Wang Y, et al. Microbial succession during the transition from active to inactive stages of deep-sea hydrothermal vent sulfide chimneys. Microbiome. 2020;8(1):102. https://doi.org/10.1186/s40168-020-00851-8.
5. Reysenbach AL, St. John E, Meneghin J, et al. Complex subsurface hydrothermal fluid mixing at a submarine arc volcano supports distinct and highly diverse microbial communities. Proc Natl Acad Sci. 2020;117(51):32627–38. https://doi.org/10.1073/pnas.2019021117.
6. Zeng X, Alain K, Shao Z. Microorganisms from deep-sea hydrothermal vents. Mar Life Sci Technol. 2021;3(2):204–30. https://doi.org/10.1007/s42995-020-00086-4.
7. Zhou Z, Tran PQ, Cowley ES, Trembath-Reichert E, Anantharaman K. Diversity and ecology of microbial sulfur metabolism. Nat Rev Microbiol. 2025;23(2):122–40. https://doi.org/10.1038/s41579-024-01104-3.
8. Dick GJ. The microbiomes of deep-sea hydrothermal vents: distributed globally, shaped locally. Nat Rev Microbiol. 2019;17(5):271–83. https://doi.org/10.1038/s41579-019-0160-2.
9. Früh-Green GL, Kelley DS, Lilley MD, Cannat M, Chavagnac V, Baross JA. Diversity of magmatism, hydrothermal processes and microbial interactions at mid-ocean ridges. Nat Rev Earth Environ. 2022;3(12):852–71. https://doi.org/10.1038/s43017-022-00364-y.
10. Emerson D, Moyer CL. Neutrophilic Fe-Oxidizing *Bacteria* Are Abundant at the Loihi Seamount Hydrothermal Vents and Play a Major Role in Fe Oxide Deposition. Appl Environ Microbiol. 2002;68(6):3085–93. https://doi.org/10.1128/AEM.68.6.3085-3093.2002.
11. Feuillet N, Jorry S, Crawford WC, et al. Birth of a large volcanic edifice offshore Mayotte via lithosphere-scale dyke intrusion. Nat Geosci. 2021;14(10):787–95. https://doi.org/10.1038/s41561-021-00809-x.

12. Verdurme P, Le Losq C, Chevrel O, et al. Viscosity of crystal-free silicate melts from the active submarine volcanic chain of Mayotte. Chem Geol. 2023;620:121326. https://doi.org/10.1016/j.chemgeo.2023.121326.
13. van der Woerd J, Famin V, Humler E. Special issue *Comptes-Rendus Geoscience*: The Mayotte seismo-volcanic crisis of 2018–2021 in the eastern Comoros archipelago (Mozambique channel). Comptes Rendus Géosci. 2022;354(S2):1–6. https://doi.org/10.5802/crgeos.196.
14. Berthod C, Komorowski JC, Gurioli L, et al. Temporal magmatic evolution of the Fani Maoré submarine eruption 50 km east of Mayotte revealed by *in situ* sampling and petrological monitoring. Comptes Rendus Géosci. 2023;354(S2):195–223. https://doi.org/10.5802/crgeos.155.
15. Mastin M, Cathalot C, Fandino O, et al. Strong geochemical anomalies following active submarine eruption offshore Mayotte. Chem Geol. 2023;640:121739. https://doi.org/10.1016/j.chemgeo.2023.121739.
16. Gamo T, Okamura K, Charlou JL, et al. Acidic and sulfate-rich hydrothermal fluids from the Manus back-arc basin. Papua New Guinea Geol. 1997;25(2):139–42. https://doi.org/10.1130/0091-7613(1997)025%3c0139:AASRHF%3e2.3.CO;2.
17. Fouquet Y, Pelleter E, Konn C, et al. Volcanic and hydrothermal processes in submarine calderas: The Kulo Lasi example (SW Pacific). Ore Geol Rev. 2018;99:314–43. https://doi.org/10.1016/j.oregeorev.2018.06.006.
18. Dekov VM, Koschinsky A, Yamanaka T, et al. Native sulfur at the seafloor: Composition and origin. Chem Geol. 2024;668:122295. https://doi.org/10.1016/j.chemgeo.2024.122295.
19. Gena K, Mizuta T, Ishiyama D, Urabe T. Acid-sulphate Type Alteration and Mineralization in the Desmos Caldera, Manus Back-arc Basin. Papua New Guinea Resource Geol. 2001;51(1):31–44. https://doi.org/10.1111/j.1751-3928.2001.tb00079.x.
20. de Ronde CEJ, Massoth GJ, Butterfield DA, et al. Submarine hydrothermal activity and gold-rich mineralization at Brothers Volcano, Kermadec Arc. New Zealand Miner Deposita. 2011;46(5):541–84. https://doi.org/10.1007/s00126-011-0345-8.
21. Herzig P, Hannington M, Arribas A. Sulfur isotopic composition of hydrothermal precipitates from the Lau back-arc: Implications for magmatic contributions to seafloor hydrothermal systems. Miner Deposita. 1998;33:226–37. https://doi.org/10.1007/s001260050143.
22. Lee H, Choi Y, Han JH, Lee SD, Park S, Choi JH. Submarine volcanic microbiota record three volcano-induced tsunamis. Commun Earth Environ. 2024;5(1):1–8. https://doi.org/10.1038/s43247-024-01443-2.
23. Flores GE, Campbell JH, Kirshtein JD, et al. Microbial community structure of hydrothermal deposits from geochemically different vent fields along the Mid-Atlantic Ridge. Environ Microbiol. 2011;13(8):2158–71. https://doi.org/10.1111/j.1462-2920.2011.02463.x.
24. Campbell BJ, Engel AS, Porter ML, Takai K. The versatile *ε-proteobacteria*: key players in sulphidic habitats. Nat Rev Microbiol. 2006;4(6):458–68. https://doi.org/10.1038/nrmicro1414.
25. Waite DW, Vanwonterghem I, Rinke C, et al. Comparative Genomic Analysis of the Class Epsilonproteobacteria and Proposed Reclassification to Epsilonbacteraeota (phyl. nov.). Front Microbiol. 2017;8:682. https://doi.org/10.3389/fmicb.2017.00682.
26. Molari M, Hassenrueck C, Laso-Pérez R, et al. A hydrogenotrophic *Sulfurimonas* is globally abundant in deep-sea oxygen-saturated hydrothermal plumes. Nat Microbiol. 2023;8(4):651–65. https://doi.org/10.1038/s41564-023-01342-w.
27. Wegener G, Molari M, Purser A, et al. Hydrothermal vents supporting persistent plumes and microbial chemoautotrophy at Gakkel Ridge (Arctic Ocean). Front Microbiol. 2024;15:1473822. https://doi.org/10.3389/fmicb.2024.1473822.
28. Sheik CS, Anantharaman K, Breier JA, Sylvan JB, Edwards KJ, Dick GJ. Spatially resolved sampling reveals dynamic microbial communities in rising hydrothermal plumes across a back-arc basin. ISME J. 2015;9(6):1434–45. https://doi.org/10.1038/ismej.2014.228.
29. Spietz RL, Butterfield DA, Buck NJ, Larson BI Jr, WWC. Deep-Sea Volcanic Eruptions Create Unique Chemical and Biological Linkages Between the Subsurface Lithosphere and the Oceanic Hydrosphere. Oceanography. 2018;31(1):128–35. https://doi.org/10.5670/oceanog.2018.120.
30. Emmanuel R, CATHALOT Cécile, FEUILLET Nathalie. GEOFLAMME cruise,Pourquoi pas ? R/V. Published online 2021. https://doi.org/10.17600/18001297
31. Catalogue des campagnes à la mer. Accessed June 17, 2024. https://campagnes.flotteoceanographique.fr/prl?id=BFBGX-142573
32. Von Damm KL, Edmond JM, Grant B, Measures CI, Walden B, Weiss RF. Chemistry of submarine hydrothermal solutions at 21 °N, East Pacific Rise. Geochim Cosmochim Acta. 1985;49(11):2197–220. https://doi.org/10.1016/0016-7037(85)90222-4.
33. Rouxel O, Toner B, Germain Y, Glazer B. Geochemical and iron isotopic insights into hydrothermal iron oxyhydroxide deposit formation at Loihi Seamount. Geochim Cosmochim Acta. 2018;220:449–82. https://doi.org/10.1016/j.gca.2017.09.050.
34. Cline JD. Spectrophotometric Determination of Hydrogen Sulfide in Natural Waters1. Limnol Oceanogr. 1969;14(3):454–8. https://doi.org/10.4319/lo.1969.14.3.0454.
35. Craddock PR, Rouxel OJ, Ball LA, Bach W. Sulfur isotope measurement of sulfate and sulfide by high-resolution MC-ICP-MS. Chem Geol. 2008;253(3):102–13. https://doi.org/10.1016/j.chemgeo.2008.04.017.
36. Charbonnier, F., G. Erauso, T. Barbeyron, D. Prieur, and P. Forterre. Purification of plasmids from thermophilic and hyper-thermophilic archaebacteria. In F. T. Robb, K. R. Sowers, S. DasSarma, A. R. Place, H. J. Schreier, and E. M. Fleischmann (ed.), Archaea: a laboratory manual, in press. Cold Spring Harbor Laboratory Press, Cold Spring Harbor, N.Y.
37. Andrews S. FastQC: a quality control tool for high throughput sequence data. 2010.
38. Ewels P, Magnusson M, Lundin S, Käller M. MultiQC: summarize analysis results for multiple tools and samples in a single report. Bioinformatics. 2016;32(19):3047–8. https://doi.org/10.1093/bioinformatics/btw354.
39. Eren AM, Vineis JH, Morrison HG, Sogin ML. A Filtering Method to Generate High Quality Short Reads Using Illumina Paired-End Technology. Jordan IK, ed. PLoS ONE. 2013;8(6):e66643. https://doi.org/10.1371/journal.pone.0066643.
40. Minoche AE, Dohm JC, Himmelbauer H. Evaluation of genomic high-throughput sequencing data generated on Illumina HiSeq and Genome Analyzer systems. Genome Biol. 2011;12(11):R112. https://doi.org/10.1186/gb-2011-12-11-r112.
41. Köster J, Rahmann S. Snakemake—a scalable bioinformatics workflow engine. Bioinformatics. 2012;28(19):2520–2. https://doi.org/10.1093/bioinformatics/bts480.
42. Eren AM. Community-led, integrated, reproducible multi-omics with anvi'o. Nat Microbiol. 2021;6(1):3–6. https://doi.org/10.1038/s41564-020-00834-3.
43. Shaiber A, Willis AD, Delmont TO, et al. Functional and genetic markers of niche partitioning among enigmatic members of the human oral microbiome. Genome Biol. 2020;21(1):292. https://doi.org/10.1186/s13059-020-02195-w.
44. Peng Y, Leung HCM, Yiu SM, Chin FYL. IDBA-UD: a de novo assembler for single-cell and metagenomic sequencing data with highly uneven depth. Bioinformatics. 2012;28(11):1420–8. https://doi.org/10.1093/bioinformatics/bts174.
45. Hyatt D, Chen GL, LoCascio PF, Land ML, Larimer FW, Hauser LJ. Prodigal: prokaryotic gene recognition and translation initiation site identification. BMC Bioinformatics. 2010;11(1):119. https://doi.org/10.1186/1471-2105-11-119.
46. Aramaki T, Blanc-Mathieu R, Endo H, et al. KofamKOALA: KEGG Ortholog assignment based on profile HMM and adaptive score threshold. Valencia A, ed. Bioinformatics. 2020;36(7):2251–2. https://doi.org/10.1093/bioinformatics/btz859.
47. Danecek P, Bonfield JK, Liddle J, et al. Twelve years of SAMtools and BCFtools. GigaScience. 2021;10(2):giab008. https://doi.org/10.1093/gigascience/giab008.
48. Langmead B, Trapnell C, Pop M, Salzberg SL. Ultrafast and memory-efficient alignment of short DNA sequences to the human genome. Genome Biol. 2009;10(3):R25. https://doi.org/10.1186/gb-2009-10-3-r25.
49. Kang DD, Li F, Kirton E, et al. MetaBAT 2: an adaptive binning algorithm for robust and efficient genome reconstruction from metagenome assemblies. PeerJ. 2019;7:e7359. https://doi.org/10.7717/peerj.7359.

50. Eren AM, Esen ÖC, Quince C, et al. Anvi'o: an advanced analysis and visualization platform for 'omics data. PeerJ. 2015;3:e1319. https://doi.org/10.7717/peerj.1319.
51. Parks DH, Imelfort M, Skennerton CT, Hugenholtz P, Tyson GW. CheckM: assessing the quality of microbial genomes recovered from isolates, single cells, and metagenomes. Genome Res. 2015;25(7):1043–55. https://doi.org/10.1101/gr.186072.114.
52. Chaumeil PA, Mussig AJ, Hugenholtz P, Parks DH. GTDB-Tk v2: memory friendly classification with the genome taxonomy database. Bioinformatics. 2022;38(23):5315–6. https://doi.org/10.1093/bioinformatics/btac672.
53. Chalita M, Kim YO, Park S, et al. EzBioCloud: a genome-driven database and platform for microbiome identification and discovery. Int J Syst Evol Microbiol. 2024;74(6):006421. https://doi.org/10.1099/ijsem.0.006421.
54. Gruber-Vodicka HR, Seah BKB, Pruesse E. phyloFlash: Rapid Small-Subunit rRNA Profiling and Targeted Assembly from Metagenomes. Arumugam M, ed. mSystems. 2020;5(5):e00920-20. https://doi.org/10.1128/mSystems.00920-20.
55. Quast C, Pruesse E, Yilmaz P, et al. The SILVA ribosomal RNA gene database project: improved data processing and web-based tools. Nucleic Acids Res. 2012;41(D1):D590–6. https://doi.org/10.1093/nar/gks1219.
56. Bushnell B. BBMap: A Fast, Accurate, Splice-Aware Aligner. Published online March 19, 2014. Accessed June 5, 2024. https://escholarship.org/uc/item/1h3515gn
57. Prjibelski A, Antipov D, Meleshko D, Lapidus A, Korobeynikov A. Using SPAdes De Novo Assembler. Curr Protocols Bioinform. 2020;70(1):e102. https://doi.org/10.1002/cpbi.102.
58. McMurdie PJ, Holmes S. phyloseq: An R Package for Reproducible Interactive Analysis and Graphics of Microbiome Census Data. PLoS ONE. 2013;8(4):e61217. https://doi.org/10.1371/journal.pone.0061217.
59. Wickham H. Data Analysis. In: Wickham H, ed. *Ggplot2: Elegant Graphics for Data Analysis*. Springer International Publishing; 2016:189–201. https://doi.org/10.1007/978-3-319-24277-4_9
60. Lee MD. GToTree: a user-friendly workflow for phylogenomics. Bioinformatics. 2019;35(20):4162–4. https://doi.org/10.1093/bioinformatics/btz188.
61. Edgar RC. Muscle5: High-accuracy alignment ensembles enable unbiased assessments of sequence homology and phylogeny. Nat Commun. 2022;13(1):6968. https://doi.org/10.1038/s41467-022-34630-w.
62. Nguyen LT, Schmidt HA, von Haeseler A, Minh BQ. IQ-TREE: A Fast and Effective Stochastic Algorithm for Estimating Maximum-Likelihood Phylogenies. Mol Biol Evol. 2015;32(1):268–74. https://doi.org/10.1093/molbev/msu300.
63. Li G, Rabe KS, Nielsen J, Engqvist MKM. Machine Learning Applied to Predicting Microorganism Growth Temperatures and Enzyme Catalytic Optima. ACS Synth Biol. 2019;8(6):1411–20. https://doi.org/10.1021/acssynbio.9b00099.
64. Capella-Gutiérrez S, Silla-Martínez JM, Gabaldón T. trimAl: a tool for automated alignment trimming in large-scale phylogenetic analyses. Bioinformatics. 2009;25(15):1972–3. https://doi.org/10.1093/bioinformatics/btp348.
65. Seemann T. Prokka: rapid prokaryotic genome annotation. Bioinformatics. 2014;30(14):2068–9. https://doi.org/10.1093/bioinformatics/btu153.
66. Hanke A, Hamann E, Sharma R, et al. Recoding of the stop codon UGA to glycine by a BD1–5/SN-2 bacterium and niche partitioning between Alpha- and Gammaproteobacteria in a tidal sediment microbial community naturally selected in a laboratory chemostat. Front Microbiol. 2014;5:231. https://doi.org/10.3389/fmicb.2014.00231.
67. Kanehisa M, Sato Y, Kawashima M, Furumichi M, Tanabe M. KEGG as a reference resource for gene and protein annotation. Nucleic Acids Res. 2016;44(D1):D457–62. https://doi.org/10.1093/nar/gkv1070.
68. Garber AI, Nealson KH, Okamoto A, et al. FeGenie: A Comprehensive Tool for the Identification of Iron Genes and Iron Gene Neighborhoods in Genome and Metagenome Assemblies. Front Microbiol. 2020;11:37. https://doi.org/10.3389/fmicb.2020.00037.
69. Neukirchen S, Sousa FL. DiSCo: a sequence-based type-specific predictor of Dsr-dependent dissimilatory sulphur metabolism in microbial data. Microb Genomics. 2021;7(7):000603. https://doi.org/10.1099/mgen.0.000603.
70. Wasmund K, Mußmann M, Loy A. The life sulfuric: microbial ecology of sulfur cycling in marine sediments. Environ Microbiol Rep. 2017;9(4):323–44. https://doi.org/10.1111/1758-2229.12538.
71. van Vliet DM, von Meijenfeldt FAB, Dutilh BE, et al. The bacterial sulfur cycle in expanding dysoxic and euxinic marine waters. Environ Microbiol. 2021;23(6):2834–57. https://doi.org/10.1111/1462-2920.15265.
72. Finster K, Liesack W, Thamdrup B. Elemental Sulfur and Thiosulfate Disproportionation by Desulfocapsa sulfoexigens sp. nov., a New Anaerobic Bacterium Isolated from Marine Surface Sediment. Appl Environ Microbiol. 1998;64(1):119–25. https://doi.org/10.1128/AEM.64.1.119-125.1998.
73. Jarvis B, Wilrich C, Wilrich P-T. Reconsideration of the derivation of Most Probable Numbers, their standard deviations, confidence bounds and rarity values. J Appl Microbiol. 2010;109(5):1660–7. https://doi.org/10.1111/j.1365-2672.2010.04792.x.
74. Webster G, Rinna J, Roussel EG, Fry JC, Weightman AJ, Parkes RJ. Prokaryotic functional diversity in different biogeochemical depth zones in tidal sediments of the Severn Estuary, UK, revealed by stable-isotope probing. FEMS Microbiol Ecol. 2010;72(2):179–97. https://doi.org/10.1111/j.1574-6941.2010.00848.x.
75. Roussel EG, Cragg BA, Webster G, et al. Complex coupled metabolic and prokaryotic community responses to increasing temperatures in anaerobic marine sediments: critical temperatures and substrate changes. FEMS Microbiol Ecol. 2015;91(8):fiv084. https://doi.org/10.1093/femsec/fiv084.
76. Cord-Ruwisch R. A quick method for the determination of dissolved and precipitated sulfides in cultures of sulfate-reducing *bacteria*. J Microbiol Methods. 1985;4(1):33–6. https://doi.org/10.1016/0167-7012(85)90005-3.
77. Borrell N, Acinas SG, Figueras MJ, Martínez-Murcia AJ. Identification of Aeromonas clinical isolates by restriction fragment length polymorphism of PCR-amplified 16S rRNA genes. J Clin Microbiol. 1997;35(7):1671–4. https://doi.org/10.1128/jcm.35.7.1671-1674.1997.
78. Sasoh M, Masai E, Ishibashi S, et al. Characterization of the Terephthalate Degradation Genes of Comamonas sp Strain E6. App Environ Microbiol. 2006;72(3):1825–32. https://doi.org/10.1128/AEM.72.3.1825-1832.2006.
79. Teske A, Hinrichs KU, Edgcomb V, et al. Microbial Diversity of Hydrothermal Sediments in the Guaymas Basin: Evidence for Anaerobic Methanotrophic Communities. Appl Environ Microbiol. 2002;68(4):1994–2007. https://doi.org/10.1128/AEM.68.4.1994-2007.2002.
80. Guindon S, Dufayard JF, Lefort V, Anisimova M, Hordijk W, Gascuel O. New Algorithms and Methods to Estimate Maximum-Likelihood Phylogenies: Assessing the Performance of PhyML 3.0. System Biol. 2010;59(3):307–21. https://doi.org/10.1093/sysbio/syq010.
81. Lupton J, Butterfield D, Lilley M, et al. Submarine venting of liquid carbon dioxide on a Mariana Arc volcano. *Geochemistry, Geophysics, Geosystems*. 2006;7(8). https://doi.org/10.1029/2005GC001152
82. Chauvel C, Inglis EC, Gutierrez P, Luu TH, Burckel P, Besson P. Fani Maoré, a new "young HIMU" volcano with extreme geochemistry. Earth Planet Sci Lett. 2024;626:118529. https://doi.org/10.1016/j.epsl.2023.118529.
83. Seewald JS, Reeves EP, Bach W, et al. Geochemistry of hot-springs at the SuSu Knolls hydrothermal field, Eastern Manus Basin: Advanced argillic alteration and vent fluid acidity. Geochim Cosmochim Acta. 2019;255:25–48. https://doi.org/10.1016/j.gca.2019.03.034.
84. Kürzinger V, Diehl A, Pereira SI, Strauss H, Bohrmann G, Bach W. Sulfur formation associated with coexisting sulfide minerals in the Kemp Caldera hydrothermal system. Scotia Sea Chem Geol. 2022;606:120927. https://doi.org/10.1016/j.chemgeo.2022.120927.
85. Dottin JW III, Labidi J, Jackson MG, Farquhar J. Sulfur Isotope Evidence for a Geochemical Zonation of the Samoan Mantle Plume. Geochem, Geophys, Geosyst. 2021;22(6):e2021GC009816. https://doi.org/10.1029/2021GC009816.
86. Labidi J, Cartigny P, Hamelin C, Moreira M, Dosso L. Sulfur isotope budget (32S, 33S, 34S and 36S) in Pacific-Antarctic ridge basalts: A record of mantle source heterogeneity and hydrothermal sulfide assimilation. Geochim Cosmochim Acta. 2014;133:47–67. https://doi.org/10.1016/j.gca.2014.02.023.
87. Ferrera I, Arrieta JM, Sebastián M, Fraile-Nuez E. Microbial Communities Surrounding an Underwater Volcano Near the Island of El Hierro (Canary Islands). In: González PJ, ed. *El Hierro Island*. Springer International Publishing; 2023:203–216. https://doi.org/10.1007/978-3-031-35135-8_10

88. Huber JA, Butterfield DA, Baross JA. Bacterial diversity in a subseafloor habitat following a deep-sea volcanic eruption. FEMS Microbiol Ecol. 2003;43(3):393–409. https://doi.org/10.1111/j.1574-6941.2003.tb01080.x.
89. Thomas F, Hehemann JH, Rebuffet E, Czjzek M, Michel G. Environmental and Gut *Bacteroidetes*: The Food Connection. Front Microbiol. 2011;2:93. https://doi.org/10.3389/fmicb.2011.00093.
90. Bowers RM, Kyrpides NC, Stepanauskas R, et al. Minimum information about a single amplified genome (MISAG) and a metagenome-assembled genome (MIMAG) of *bacteria and archaea*. Nat Biotechnol. 2017;35(8):725–31. https://doi.org/10.1038/nbt.3893.
91. Finster K, Liesack W, Tindall BJ. Sulfurospirillum arcachonense sp. nov., a New Microaerophilic Sulfur-Reducing Bacterium. Int J Syst Evol Microbiol. 1997;47(4):1212–7. https://doi.org/10.1099/00207713-47-4-1212.
92. Liesack W, Finster K. Phylogenetic Analysis of Five Strains of Gram-Negative, Obligately Anaerobic, Sulfur-Reducing Bacteria and Description of Desulfuromusa gen. nov., Including Desulfuromusa kysingii sp. nov., Desulfuromusa bakii sp. nov., and Desulfuromusa succinoxidans sp. nov. Int J Syst Evol Microbiol. 1994;44(4):753–8. https://doi.org/10.1099/00207713-44-4-753.
93. Inagaki F, Takai K, Kobayashi H, Nealson KH, Horikoshi K. Sulfurimonas autotrophica gen. nov., sp. nov., a novel sulfur-oxidizing ε-proteobacterium isolated from hydrothermal sediments in the Mid-Okinawa Trough. Int J System Evol Microbiol. 2003;53(6):1801–5. https://doi.org/10.1099/ijs.0.02682-0.
94. Inagaki F, Takai K, Nealson KH, Horikoshi K. Sulfurovum lithotrophicum gen. nov., sp. nov., a novel sulfur-oxidizing chemolithoautotroph within the ε-Proteobacteria isolated from Okinawa Trough hydrothermal sediments. Int J Syst Evol Microbiol. 2004;54(5):1477–82. https://doi.org/10.1099/ijs.0.03042-0.
95. Galushko A, Kuever J. Bilophila. In: *Bergey's Manual of Systematics of Archaea and Bacteria*. John Wiley & Sons, Ltd; 2019:1–5. https://doi.org/10.1002/9781118960608.gbm01034.pub2
96. Scheuner C, Tindall BJ, Lu M, et al. Complete genome sequence of *Planctomyces brasiliensis* type strain (DSM 5305^T), phylogenomic analysis and reclassification of *Planctomycetes* including the descriptions of *Gimesia* gen. nov., *Planctopirus* gen. nov. and *Rubinisphaera* gen. nov. and emended descriptions of the order *Planctomycetales* and the family *Planctomycetaceae*. Stand Genomic Sci. 2014;9(1):10. https://doi.org/10.1186/1944-3277-9-10.
97. Florentino AP, Weijma J, Stams AJM, Sánchez-Andrea I. Ecophysiology and Application of Acidophilic Sulfur-Reducing Microorganisms. In: Rampelotto PH, ed. *Biotechnology of Extremophiles: Advances and Challenges*. Springer International Publishing; 2016:141–175. https://doi.org/10.1007/978-3-319-13521-2_5
98. Dubinina G, Savvichev A, Orlova M, Gavrish E, Verbarg S, Grabovich M. Beggiatoa leptomitoformis sp. nov., the first freshwater member of the genus capable of chemolithoautotrophic growth. Int J Syst Evol Microbiol. 2017;67(2):197–204. https://doi.org/10.1099/ijsem.0.001584.
99. Gureeva MV, Belousova EV, Dubinina GA, Novikov AA, Kopitsyn DS, Grabovich MY. Thioflexithrix psekupsensis gen. nov., sp. nov., a filamentous gliding sulfur bacterium from the family Beggiatoaceae. Int J Syst Evol Microbiol. 2019;69(3):798–804. https://doi.org/10.1099/ijsem.0.003240.
100. Larkin JM, Shinabarger DL. Characterization of *Thiothrix nivea*. Int J Syst Bacteriol. 1983;33(4):841–6. https://doi.org/10.1099/00207713-33-4-841.
101. Tavormina PL, Hatzenpichler R, McGlynn S, et al. Methyloprofundus sedimenti gen. nov., sp. nov., an obligate methanotroph from ocean sediment belonging to the 'deep sea-1' clade of marine methanotrophs. Int J Syst Evol Microbiol. 2015;65(Pt_1):251–9. https://doi.org/10.1099/ijs.0.062927-0.
102. Le Moine Bauer S, Roalkvam I, Steen IH, Dahle H. Lutibacter profundi sp. nov., isolated from a deep-sea hydrothermal system on the Arctic Mid-Ocean Ridge and emended description of the genus Lutibacter. Int J Syst Evol Microbiol. 2016;66(7):2671–7. https://doi.org/10.1099/ijsem.0.001105.
103. Han B, Kim M, Lee KE, Lee BH, Lee EY, Park SJ. Formosa sediminum sp. nov., a starch-degrading bacterium isolated from marine sediment. Int J System Evol Microbiol. 2020;70(3):2008–15. https://doi.org/10.1099/ijsem.0.004012.
104. Zhong YL, Zhang R, Zhang XY, Yu LX, Zhao MF, Du ZJ. Psychroflexus maritimus sp. nov., isolated from coastal sediment. Arch Microbiol. 2020;202(8):2127–33. https://doi.org/10.1007/s00203-020-01933-9.
105. Xie S, Wang S, Li D, et al. Sulfurovum indicum sp. nov., a novel hydrogen- and sulfur-oxidizing chemolithoautotroph isolated from a deep-sea hydrothermal plume in the Northwestern Indian Ocean. Int J Syst Evol Microbiol. 2021;71(3):004748. https://doi.org/10.1099/ijsem.0.004748.
106. Wang S, Jiang L, Cui L, Alain K, Xie S, Shao Z. Transcriptome analysis of cyclooctasulfur oxidation and reduction by the neutrophilic chemolithoautotrophic *Sulfurovum indicum* from deep-sea hydrothermal ecosystems. Antioxidants. 2023;12(3):627. https://doi.org/10.3390/antiox12030627.
107. Pjevac P, Kamyshny A Jr, Dyksma S, Mußmann M. Microbial consumption of zero-valence sulfur in marine benthic habitats. Environ Microbiol. 2014;16(11):3416–30. https://doi.org/10.1111/1462-2920.12410.
108. Han Y, Perner M. The globally widespread genus *Sulfurimonas*: versatile energy metabolisms and adaptations to redox clines. Front Microbiol. 2015;6:989. https://doi.org/10.3389/fmicb.2015.00989.
109. Wang S, Jiang L, Zhao Z, et al. Chemolithoautotrophic diazotrophs dominate dark nitrogen fixation in mangrove sediments. ISME J. 2024;18(1):119. https://doi.org/10.1093/ismejo/wrae119.
110. Santos Correa S, Schultz J, Lauersen KJ, Soares RA. Natural carbon fixation and advances in synthetic engineering for redesigning and creating new fixation pathways. J Adv Res. 2023;47:75–92. https://doi.org/10.1016/j.jare.2022.07.011.
111. Torelli M, Battani A, Pillot D, et al. Origin and preservation conditions of organic matter in the Mozambique Channel: evidence for widespread oxidation processes in the deep-water domains. Mar Geol. 2021;440:106589. https://doi.org/10.1016/j.margeo.2021.106589.
112. Sievert SM, Scott KM, Klotz MG, et al. Genome of the *Epsilonproteobacterial* Chemolithoautotroph *Sulfurimonas denitrificans*. Appl Environ Microbiol. 2008;74(4):1145–56. https://doi.org/10.1128/AEM.01844-07.
113. McAllister SM, Polson SW, Butterfield DA, Glazer BT, Sylvan JB, Chan CS. Validating the Cyc2 neutrophilic iron oxidation pathway using meta-omics of *Zetaproteobacteria* iron mats at marine hydrothermal vents. mSystems. 2020;5(1):e00553-19. https://doi.org/10.1128/mSystems.00553-19.
114. Castelle CJ, Roger M, Bauzan M, et al. The aerobic respiratory chain of the acidophilic archaeon *Ferroplasma acidiphilum*: a membrane-bound complex oxidizing ferrous iron. Biochim Biophys Acta. 2015;1847(8):717–28. https://doi.org/10.1016/j.bbabio.2015.04.006.
115. Bird LJ, Bonnefoy V, Newman DK. Bioenergetic challenges of microbial iron metabolisms. Trends Microbiol. 2011;19(7):330–40. https://doi.org/10.1016/j.tim.2011.05.001.
116. Mendoza-Cózatl D, Loza-Tavera H, Hernández-Navarro A, Moreno-Sánchez R. Sulfur assimilation and glutathione metabolism under cadmium stress in yeast, protists and plants. FEMS Microbiol Rev. 2005;29(4):653–71. https://doi.org/10.1016/j.femsre.2004.09.004.
117. Vuilleumier S, Pagni M. The elusive roles of bacterial glutathione S-transferases: new lessons from genomes. Appl Microbiol Biotechnol. 2002;58(2):138–46. https://doi.org/10.1007/s00253-001-0836-0.
118. Peters JW, Schut GJ, Boyd ES, et al. [FeFe]- and [NiFe]-hydrogenase diversity, mechanism, and maturation. Biochimica et Biophysica Acta (BBA). Mol Cell Res. 2015;1853(6):1350–69. https://doi.org/10.1016/j.bbamcr.2014.11.021.
119. Tian R, Ning D, He Z, et al. Small and mighty: adaptation of superphylum Patescibacteria to groundwater environment drives their genome simplicity. Microbiome. 2020;8(1):51. https://doi.org/10.1186/s40168-020-00825-w.
120. Zhou Z, St. John E, Anantharaman K, Reysenbach AL. Global patterns of diversity and metabolism of microbial communities in deep-sea hydrothermal vent deposits. Microbiome. 2022;10(1):241. https://doi.org/10.1186/s40168-022-01424-7.
121. Nascimento Lemos L, Manoharan L, William Mendes L, Monteiro Venturini A, Satler Pylro V, Tsai SM. Metagenome assembled-genomes reveal similar functional profiles of CPR/*Patescibacteria* phyla in soils. Environ Microbiol Rep. 2020;12(6):651–5. https://doi.org/10.1111/1758-2229.12880.
122. Salman-Carvalho V, Fadeev E, Joye SB, Teske A. How clonal is clonal? Genome plasticity across multicellular segments of a "*Candidatus*

Marithrix sp." filament from sulfidic, briny seafloor sediments in the Gulf of Mexico. *Front Microbiol*. 2016;7. https://doi.org/10.3389/fmicb.2016.01173
123. Mußmann M, Pjevac P, Krüger K, Dyksma S. Genomic repertoire of the *Woeseiaceae*/JTB255, cosmopolitan and abundant core members of microbial communities in marine sediments. ISME J. 2017;11(5):1276–81. https://doi.org/10.1038/ismej.2016.185.
124. Lahme S, Callbeck CM, Eland LE, et al. Comparison of sulfide-oxidizing *Sulfurimonas* strains reveals a new mode of thiosulfate formation in subsurface environments. Environ Microbiol. 2020;22(5):1784–800. https://doi.org/10.1111/1462-2920.14894.
125. Rees GN, Harfoot CG, Sheehy AJ. Amino acid degradation by the mesophilic sulfate-reducing bacterium *Desulfobacterium vacuolatum*. Arch Microbiol. 1997;169(1):76–80. https://doi.org/10.1007/s002030050543.
126. Slobodkin AI, Slobodkina GB. Diversity of sulfur-disproportionating microorganisms. Microbiology. 2019;88(5):509–22. https://doi.org/10.1134/S0026261719050138.
127. Allioux M, Yvenou S, Slobodkina G, et al. Genomic characterization and environmental distribution of a thermophilic anaerobe *Dissulfurirhabdus thermomarina* SH388^T involved in disproportionation of sulfur compounds in shallow sea hydrothermal vents. Microorganisms. 2020;8(8):1132. https://doi.org/10.3390/microorganisms8081132.
128. Yvenou S, Allioux M, Slobodkin A, Slobodkina G, Jebbar M, Alain K. Genetic potential of *Dissulfurimicrobium hydrothermale*, an obligate sulfur-disproportionating thermophilic microorganism. Microorganisms. 2021;10(1):60. https://doi.org/10.3390/microorganisms10010060.
129. Aronson HS, Clark CE, LaRowe DE, Amend JP, Polerecky L, Macalady JL. Sulfur disproportionating microbial communities in a dynamic, micro-oxic-sulfidic karst system. Geobiology. 2023;21(6):791–803. https://doi.org/10.1111/gbi.12574.
130. Alain K, Aronson HS, Allioux M, Yvenou S, Amend JP. Sulfur disproportionation is exergonic in the vicinity of marine hydrothermal vents. Environ Microbiol. 2022;24(5):2210–9. https://doi.org/10.1111/1462-2920.15975.
131. Wu B, Liu F, Fang W, et al. Microbial sulfur metabolism and environmental implications. Sci Total Environ. 2021;778:146085. https://doi.org/10.1016/j.scitotenv.2021.146085.
132. Wang S, Jiang L, Hu Q, Liu X, Yang S, Shao Z. Elemental sulfur reduction by a deep-sea hydrothermal vent Campylobacterium Sulfurimonas sp. NW10. Environ Microbiol. 2021;23(2):965–79. https://doi.org/10.1111/1462-2920.15247.
133. Wang S, Jiang L, Hu Q, et al. Characterization of Sulfurimonas hydrogeniphila sp. nov., a Novel Bacterium Predominant in Deep-Sea Hydrothermal Vents and Comparative Genomic Analyses of the Genus Sulfurimonas. Front Microbiol. 2021;12:626705. https://doi.org/10.3389/fmicb.2021.626705.
134. Wang S, Jiang L, Xie S, et al. Disproportionation of inorganic sulfur compounds by mesophilic chemolithoautotrophic *Campylobacterota*. mSystems. 2022;8(1):e00954-22. https://doi.org/10.1128/msystems.00954-22.
135. Takai K, Nealson KH, Horikoshi K. Hydrogenimonas thermophila gen. nov., sp. nov., a novel thermophilic, hydrogen-oxidizing chemolithoautotroph within the ε-Proteobacteria, isolated from a black smoker in a Central Indian Ridge hydrothermal field. Int J Syst Evol Microbiol. 2004;54(1):25–32. https://doi.org/10.1099/ijs.0.02787-0.
136. Grote J, Jost G, Labrenz M, Herndl GJ, Jürgens K. *Epsilonproteobacteria* represent the major portion of chemoautotrophic *bacteria* in sulfidic waters of pelagic redoxclines of the Baltic and Black Seas. Appl Environ Microbiol. 2008;74(24):7546–51. https://doi.org/10.1128/AEM.01186-08.
137. Sorokin DYU, Tourova TP, Panteleeva AN, Muyzer G. Desulfonatronobacter acidivorans gen. nov., sp. nov. and Desulfobulbus alkaliphilus sp. nov., haloalkaliphilic heterotrophic sulfate-reducing bacteria from soda lakes. Int J Syst Evol Microbiol. 2012;62(9):2107–13. https://doi.org/10.1099/ijs.0.029777-0.
138. El Houari A, Ranchou-Peyruse M, Ranchou-Peyruse A, et al. Desulfobulbus oligotrophicus sp. nov., a sulfate-reducing and propionate-oxidizing bacterium isolated from a municipal anaerobic sewage sludge digester. Int J Syst Evol Microbiol. 2017;67(2):275–81. https://doi.org/10.1099/ijsem.0.001615.
139. Hashimoto Y, Shimamura S, Tame A, et al. Physiological and comparative proteomic characterization of *Desulfolithobacter dissulfuricans* gen. nov., sp. nov., a novel mesophilic, sulfur-disproportionating chemolithoautotroph from a deep-sea hydrothermal vent. *Front Microbiol*. 2022;13. https://doi.org/10.3389/fmicb.2022.1042116
140. Nisman B. The Stickland reaction. Bacteriol Rev. 1954;18(1):16–42. https://doi.org/10.1128/br.18.1.16-42.1954.
141. Mall A, Sobotta J, Huber C, et al. Reversibility of citrate synthase allows autotrophic growth of a thermophilic bacterium. Science. 2018;359(6375):563–7. https://doi.org/10.1126/science.aao2410.
142. Steffens L, Pettinato E, Steiner TM, et al. High CO_2 levels drive the TCA cycle backwards towards autotrophy. Nature. 2021;592(7856):784–8. https://doi.org/10.1038/s41586-021-03456-9.
143. Lim SJ, Thompson LR, Young CM, Gaasterland T, Goodwin KD. Dominance of *Sulfurospirillum* in metagenomes associated with the methane ice worm (*Sirsoe methanicola*). Appl Environ Microbiol. 2022;88(15):e00290-e322. https://doi.org/10.1128/aem.00290-22.

Publisher's Note